Stabilised FEM for Degenerate Convex Minimisation Problems under Weak Regularity Assumptions

Wolfgang Boiger * Carsten Carstensen *

The discretisation of degenerate convex minimisation problems experiences numerical difficulties with a singular or nearly singular Hessian matrix. Some discrete analog of the surface energy in microstrucures is added to the energy functional to define a stabilisation technique. This paper proves (a) strong convergence of the stress even without any smoothness assumption for a class of stabilised degenerate convex minimisation problems. Given the limitted a priori error control in those cases, the sharp a posteriori error control is of even higher relevance. This paper derives (b) guaranteed a posteriori error control via some equilibration technique which does not rely on the strict Galerkin orthogonality of the unperturbed problem. In the presence of L^2 control in the original minimisation problem, some realistic model scenario with piecewise smooth exact solution allows for strong convergence of the gradients plus refined a posteriori error estimates. This paper presents (c) an improved a posteriori error control in this interface problem and so narrows the efficiency reliability gap. Numerical experiments illustrate the theoretical convergence rates for uniform and adaptive mesh-refinements and the improved a posteriori error control for four benchmark examples in the computational microstructures.

1 Introduction

Infimising sequences of variational problems with non-quasiconvex energy densities, in general, develop finer and finer oscillations with no classical limit in Sobolev function spaces called microstructure [12, 23, 17, 20, 30, 3]. Those oscillations cause difficulty to numerical methods because fine grids are necessary to resolve such oscillations which results in ineffective and tricky mesh-depending computations. Strong convergence of gradients of infimising sequences of the non-quasiconvex problem is impossible.

Relaxation techniques replace the nonconvex energy density by its (semi-)convex hull and lead to a macroscopic model. Since the convexified energy density obtained by this method, in

*Department of Mathematics, Humboldt-Universität zu Berlin, Unter den Linden 6, 10099 Berlin, Germany, and Department of Computational Science and Engineering, Yonsei University, 120-749 Seoul, Korea; supported by the Deutsche Forschungsgemeinschaft (DFG) through the RTG 1128 and the Research Group 797 (Microplast) as well as by the Berlin Mathematical School (BMS)

general, lacks strict convexity, numerical algorithms might encounter situations where the Hessian matrix is singular. For instance, the Newton minimisation algorithm fails on the convexified three-well problem of Subsection 6.4 below. Applications of relaxation techniques include models in computational microstructure [3, 30, 18], some optimal design problems [5, 26], the nonlinear Laplacian [15], and elastoplasticity [12].

Stabilisation techniques regularise the energy term by an additional positive semidefinite stabilisation function. The paper [7] discusses several choices of such stabilisation functions for P_1 conforming finite elements and quasiuniform meshes. It turns out that stabilisation can ensure strong convergence of the strain approximations under particular circumstances. An particular stabilisation in [9] leads to strong convergence even on unstructured grids but is still restricted to unrealistically smooth solutions. This paper studies the stabilisation technique of [9] and addresses the question of convergence (i) without extra regularity assumptions and (ii) in a realistic scenario called model interface problem.

Throughout this introduction, the convex energy functional assumes the form

$$E(v) := \int_\Omega W(\mathrm{D}v(x))\,\mathrm{d}x + \text{lower-order terms in } v \in H^1_0(\Omega).$$

Assume that W is convex with quadratic growth so that there exist minimisers $u \in H^1_0(\Omega)$; below p-th order growth is included while $p = 2$ throughout this simplifying introduction. Given a sequence of shape-regular triangulations $(\mathcal{T}_\ell)_{\ell\in\mathbb{N}_0}$ [22], let u_ℓ minimise the stabilised discrete energy

$$E_\ell(v_\ell) := E(v_\ell) + \frac{1}{2}|||v_\ell|||^2_\ell \text{ with } |||v_\ell|||^2_\ell := H^2_\ell \sum_{F\in\mathcal{F}_\ell(\Omega)} h_F^{-1}\,\|[\mathrm{D}v_\ell]_F\|^2_{L^2(F)}$$

amongst all conforming P_1 finite element functions v_ℓ on $\mathcal{T}_\ell$, where $[\mathrm{D}v_\ell]_F$ is the jump of the gradient $\mathrm{D}v_\ell$ along the interior side F, written $F \in \mathcal{F}_\ell(\Omega)$, and $H_\ell := \max_T h_T$ is the maximal diameter h_T of all simplices $T \in \mathcal{T}_\ell$.

Section 3 verifies, for some problem-dependent $\beta \geqslant 0$, the strong convergence of the discrete solution u_ℓ and its stress $\sigma_\ell := \mathrm{D}W(\mathrm{D}u_\ell)$ to their respective continuous conterparts,

$$\|\sigma - \sigma_\ell\|^2_{L^2(\Omega)} + \beta\,\|u - u_\ell\|^2_{L^2(\Omega)} + |||u_\ell|||^2_\ell \to 0 \text{ as } \ell \to \infty.$$

Section 4 presents an a posteriori error bound. For the L^2 projection Π_ℓ onto the space of piecewise P_0 functions, any Raviart-Thomas function $\tau_\ell \in RT_0(\mathcal{T}_\ell)$ satisfies

$$\|\sigma - \sigma_\ell\|^2_{L^2(\Omega)} \lesssim \left(\|\sigma_\ell - \tau_\ell\|_{L^2(\Omega)} + \|\Pi_\ell f + \operatorname{div}\tau_\ell\|_{L^2(\Omega)} + \operatorname{osc}_{\ell,2}(f)\right)\|u - u_\ell\|_{H^1(\Omega)}.$$

This error bound holds for any discrete displacement u_ℓ that satisfies the boundary conditions; the point is that inexact solve is included — there is no Galerkin orthogonality required. The drawback is to minimise the expression on the right-hand side with respect to τ_ℓ in order to obtain a sharp error bound. This is a selection: degenerate convex minimisation problems do not allow for a control of $\|u - u_\ell\|_{H^1(\Omega)}$ and may even face multiple exact or discrete solutions while the discrete minimum of E_ℓ is unique. However, in some results of this paper, either W or the lower-order terms lead to some control over $\|u - u_\ell\|_{L^2(\Omega)}$ and the selection via stabilisation is correct.

Phase transition problems motivate the investigation of scenarios with a smooth solution u up to a one-dimensional interface $\Gamma \subset \overline{\Omega}$ [14]. Section 5 proves that such problems allow even for strong convergence of the gradients for any unique solution u in $W^{1,\infty}(\Omega) \cap H^2(\Omega\backslash\Gamma)$ [21].

This result also leads to an improvement of the a posteriori error control of the discrete stresses and narrows the efficiency-reliability gap; the efficiency-reliability gap is the difference of the convergence rates of the guaranteed upper a posteriori error bound and the guaranteed lower a posteriori error bound.

Section 6 complements the theoretical findings with numerical experiments to provide empirical evidence of the improved error control. The stabilisation technique competes in four benchmark examples, with and without known exact solution, for uniform and two different mesh-refining algorithms for the explicit residual-based error estimator of [18] and with an averaging-type error estimator of [14, (1.11)]. The optimistic statement that the adaptive convergence rates are always superior to uniform discretisations appears to be incorrect in computational microstructures and future research on adaptive stabilised computation of degenerate minimisation algorithms far beyond [12] appears necessary.

Standard notation on Lebesgue and Sobolev spaces is employed throughout this paper and $a \lesssim b$ abbreviates $a \leqslant Cb$ with some generic constant $0 < C < \infty$ independent of crucial parameters (like the mesh-size on level ℓ); $a \approx b$ means $a \lesssim b \lesssim a$.

2 Model Problem, Discretisation and Stabilisation

Based on the convergence results for unstructured grids, this paper will develop reliable error estimators for a class of stabilised convex minimisation problems described in the sequel. Let $\Omega \subset \mathbb{R}^n$ be a bounded Lipshitz domain with polygonal boundary for $n = 2$ or 3. Given a continuous convex energy density $W : \mathbb{R}^{m\times n} \to \mathbb{R}$, $g, f \in L^2(\Omega;\mathbb{R}^m)$, $\beta \geqslant 0$, and $v \in W^{1,p}(\Omega;\mathbb{R}^m)$ with $2 \leqslant p < \infty$ and $m = 1, \ldots, n$, the energy reads

$$E(v) := \int_\Omega \Big(W(\mathrm{D}v(x)) + \beta\,|v(x) - g(x)|^2 - f(x)\cdot v(x) \Big)\,\mathrm{d}x. \tag{2.1}$$

Throughout this paper, the energy density $W \in \mathcal{C}^1(\mathbb{R}^{m\times n};\mathbb{R})$ satisfies (2.2)–(2.3) for parameters $1 < r \leqslant 2$, $0 \leqslant s < \infty$ and $s + r + p \leqslant rp$. The *two-sided growth condition* reads

$$|F|^p - 1 \lesssim W(F) \lesssim |F|^p + 1 \ \text{ for all } F \in \mathbb{R}^{m\times n}. \tag{2.2}$$

The *convexity control* assumption reads, for all $F_1, F_2 \in \mathbb{R}^{m\times n}$,

$$|\mathrm{D}W(F_1) - \mathrm{D}W(F_2)|^r \lesssim \big(1 + |F_1|^s + |F_2|^s\big)\,(\mathrm{D}W(F_1) - \mathrm{D}W(F_2)) : (F_1 - F_2)\,. \tag{2.3}$$

Given Dirichlet data $u_D \in W^{2,p}(\Omega;\mathbb{R}^m) \cap H^2(\partial\Omega;\mathbb{R}^m)$ for the set of admissible functions $\mathcal{A} := u_D + V := u_D + W^{1,p}_0(\Omega;\mathbb{R}^m)$, the continuous (convex) model problem reads

$$\text{minimise } \ E(v) \ \text{ within } v \in \mathcal{A}. \tag{2.4}$$

A finite element approximation of (2.4) is based on a family of regular triangulations $(\mathcal{T}_\ell)_{\ell\in\mathbb{N}_0}$ of the domain Ω into simplices in the sense of Ciarlet [22] (e.g., for $n = 2$, two non-disjoint triangles of $\mathcal{T}_\ell$ share either a common edge or a common node). The set of sides $\mathcal{F}_\ell$ consists of edges (for $n = 2$) or faces (for $n = 3$) of $\mathcal{T}_\ell$ and is split into the union of the sets of all interiour sides $\mathcal{F}_\ell(\Omega)$ and of all boundary sides $\mathcal{F}_\ell(\partial\Omega)$.

For latter reference, define the diameter $h_T := \operatorname{diam} T$ of a triangle (or tetrahedron) $T \in \mathcal{T}_\ell$ and the size $h_F := \operatorname{diam} F$ of a side $F \in \mathcal{F}_\ell$. The *mesh size function* $h_\ell : \Omega \to \mathbb{R}_{>0}$ is given by

$$h_\ell(x) := \begin{cases} h_T & \text{for } x \in \operatorname{int} T \in \mathcal{T}_\ell, \\ \min\{h_F : F \in \mathcal{F}_\ell \text{ and } x \in F\} & \text{otherwise.} \end{cases}$$

The global mesh size will be abbreviated by $H_\ell := \|h_\ell\|_{L^\infty(\Omega)}$. We presume the family $(\mathcal{T}_\ell)_{\ell\in\mathbb{N}_0}$ to be *shape-regular* so that $h_F \approx h_T$ for all $T \in \mathcal{T}_\ell$, $F \in \mathcal{F}_\ell$ and $F \subset T$.

The space of $\mathcal{T}_\ell$-piecewise polynomials of degree $\leqslant k \in \mathbb{N}_0$ is $P_k(\mathcal{T}_\ell)$. The nodal interpolation $I_\ell w \in P_1(\mathcal{T}_\ell) \cap C(\overline{\Omega})$ of $w \in C(\overline{\Omega})$ is given by $I_\ell v(z) = v(z)$ for all nodes z. Let furthermore $\Pi_\ell w$ be the L^2 projection of $w \in L^2(\Omega)$ onto $P_0(\mathcal{T}_\ell)$, and $\operatorname{osc}_{\ell,q}(w) := \|h_\ell(1-\Pi_\ell)w\|_{L^q(\Omega)}$ be the oscillation of $w \in L^q(\Omega)$ for $2 \leqslant q \leqslant \infty$ with respect to the triangulation $\mathcal{T}_\ell$. Let $u_{D,\ell} = I_\ell u_D$, and

$$\mathcal{A}_\ell := u_{D,\ell} + V_\ell \text{ with } V_\ell := V \cap P_1(\mathcal{T}_\ell;\mathbb{R}^m).$$

Given a function v on Ω which is possibly discontinuous along some side $F \in \mathcal{F}_\ell(\Omega)$ shared by the two elements $T_\pm$ such that there exist traces from either sides, the *jump* of v along F reads

$$[v](x) = [v]_F(x) := \lim_{T_+ \ni y \to x} v(y) - \lim_{T_- \ni y \to x} v(y) \text{ for } x \in F.$$

The stabilisation of [9] will be used throughout this paper with $-1 < \gamma < \infty$ and

$$a_\ell(v,w) := \sum_{F\in\mathcal{F}_\ell(\Omega)} \frac{H_\ell^{1+\gamma}}{h_F} \int_F [\mathrm{D}v]_F : [\mathrm{D}w]_F \,\mathrm{d}s \text{ and } |||v|||_\ell^2 := a_\ell(v,v). \tag{2.5}$$

The stabilised discrete problem reads

$$\text{minimise } E_\ell(v) := E(v) + \frac{1}{2}a_\ell(v,v) \text{ amongst } v \in \mathcal{A}_\ell. \tag{2.6}$$

Convergence of gradients with a guaranteed convergence rate is shown in [9] under unrealistically high regularity assumptions. A comprehensive collection of the results in [9] is summarised in the following theorem.

Theorem 2.1 ([9]). *Let $u \in \mathcal{A} \cap H^{3/2+\varepsilon}(\Omega;\mathbb{R}^m)$ be some solution of (2.4) for some $\varepsilon > 0$; let p' and r' be the Hölder conjugate of p and r, $-1 < \gamma < 3$, and set*

$$\zeta := \min\{1+\gamma, r'\} \text{ for } \beta > 0 \text{ and } \zeta := \min\{1+\gamma, 2\} \text{ for } \beta = 0.$$

Then the discrete solution u_ℓ of (2.6) and the continuous and discrete stress $\sigma := \mathrm{D}W(\mathrm{D}u)$ and $\sigma_\ell := \mathrm{D}W(\mathrm{D}u_\ell)$ satisfy

$$\|\sigma - \sigma_\ell\|_{L^{p'}(\Omega)}^r + \|u - u_\ell\|_{L^2(\Omega)}^2 + |||u_\ell|||_\ell^2 + H_\ell^{(1+\gamma)/2} \|\mathrm{D}(u-u_\ell)\|_{L^2(\Omega)}^2 \lesssim H_\ell^\zeta.$$

Proof. This combines Lemma 3.5 and 4.1–4.2 plus Theorem 3.8 and 4.4 in [9]. □

3 Global Convergence

This section is devoted to the proof of a general convergence result *without* higher regularity assumptions. Let $u \in \mathcal{A}$ and $u_\ell \in \mathcal{A}_\ell$ solve the minimisation problem (2.4) and (2.6) and set $\sigma := \mathrm{D}W(\mathrm{D}u)$ and $\sigma_\ell := \mathrm{D}W(\mathrm{D}u_\ell)$. For the unstabilised approximation, the a priori error estimates of [18] plus a density argument prove convergence of

$$\|\sigma - \sigma_\ell\|_{L^{p'}(\Omega)}^r + \beta\|u - u_\ell\|_{L^2(\Omega)}^2 \to 0 \text{ as } H_\ell \to 0.$$

The point in the following result is that the stabilised approximation converges as well as $|||u_\ell|||_\ell \to 0$ even for non-smooth or non-unique minimisers.

Theorem 3.1 (Global Convergence). *Provided $u \in \mathcal{A}$, $\lim_{\ell\to\infty} H_\ell = 0$ and $\beta \geqslant 0$, it holds*

$$\|\sigma - \sigma_\ell\|^r_{L^{p'}(\Omega)} + \beta \|u - u_\ell\|^2_{L^2(\Omega)} + |||u_\ell|||^2_\ell \to 0 \text{ as } \ell \to \infty.$$

Note that this theorem permits $\beta = 0$ and then it does not guarantee the convergence of $\|u - u_\ell\|^2_{L^2(\Omega)}$. Under special circumstances, uniqueness of u and the convergence $\|u - u_\ell\|_{L^2(\Omega)} \to 0$ can be shown, e.g., in Example 3.3. The point is that even nonunique minimisers are included, the thorem holds for any of those, but then implies uniqueness.

The proof of Theorem 3.1 is based on the following lemma.

Lemma 3.2. *The errors $\delta_\ell := \sigma - \sigma_\ell$ and $e_\ell := u - u_\ell$ satisfy, for all $v_\ell \in V_\ell$, that*

$$\|\delta_\ell\|^r_{L^{p'}(\Omega)} + \beta \|e_\ell\|^2_{L^2(\Omega)} \lesssim |e_\ell - v_\ell|^{r'}_{W^{1,p}(\Omega)} + \beta \|e_\ell - v_\ell\|^2_{L^2(\Omega)} + a_\ell(u_\ell, v_\ell).$$

Proof. The minimisation problems (2.4) and (2.6) are equivalent to their respective Euler-Lagrange equations, namely for $v \in V$ and $v_\ell \in V_\ell$,

$$\int_\Omega (\sigma(x) : \mathrm{D}v(x) + 2\beta(u(x) - g(x)) \cdot v(x) - f(x) \cdot v(x)) \,\mathrm{d}x = 0; \tag{3.1}$$

$$\int_\Omega (\sigma_\ell(x) : \mathrm{D}v_\ell(x) + 2\beta(u_\ell(x) - g(x)) \cdot v_\ell(x) - f(x) \cdot v_\ell(x)) \,\mathrm{d}x + a_\ell(u_\ell, v_\ell) = 0. \tag{3.2}$$

Algebraic transformations of the difference of these two equations lead to

$$\int_\Omega \delta_\ell : \mathrm{D}e_\ell \,\mathrm{d}x + 2\beta \|e_\ell\|^2_{L^2(\Omega)} = \int_\Omega (\delta_\ell : \mathrm{D}(e_\ell - v_\ell) + 2\beta e_\ell \cdot (e_\ell - v_\ell)) \,\mathrm{d}x + a_\ell(u_\ell, v_\ell).$$

It is shown in [9, Lemma 3.5] that

$$\|\delta_\ell\|^r_{L^{p'}(\Omega)} \lesssim \int_\Omega \delta_\ell : \mathrm{D}e_\ell \,\mathrm{d}x. \tag{3.3}$$

Two Hölder inequalities on the right-hand side and absorbtions of $\|\delta_\ell\|_{L^{p'}(\Omega)}$ and $\|e_\ell\|_{L^2(\Omega)}$ eventually conclude the proof. Further details are dropped for brevity. □

Proof of Theorem 3.1. Given any positive ε, the density of smooth functions in $W^{1,p}_0(\Omega;\mathbb{R}^m)$ leads to some $v_\varepsilon \in \mathcal{D}(\Omega;\mathbb{R}^m)$ such that $\|u - u_D - v_\varepsilon\|_{W^{1,p}(\Omega)} \lesssim \varepsilon$. Hence $v_\ell := I_\ell(v_\varepsilon + u_D) - u_\ell \in V_\ell$ satisfies

$$e_\ell - v_\ell = (u - u_D - v_\varepsilon) + (1 - I_\ell)(v_\varepsilon + u_D).$$

Note that the nodal interpolation $I_\ell(v_\varepsilon + u_D)$ is well-defined since v_ε and u_D are assumed to be smooth. With [9, Lemma 3.1–3.2] it follows that

$$\|(1 - I_\ell)(v_\varepsilon + u_D)\|_{W^{1,p}(\Omega)} \lesssim H_\ell \to 0 \text{ and}$$
$$|||I_\ell(v_\varepsilon + u_D)|||^2_\ell = |||(1 - I_\ell)(v_\varepsilon + u_D)|||^2_\ell \lesssim H_\ell^{1+\gamma} \to 0 \text{ as } \ell \to \infty.$$

Since $\|\cdot\|_{L^2(\Omega)} \lesssim \|\cdot\|_{W^{1,p}(\Omega)}$, this yields some $\ell_0 \in \mathbb{N}$ such that

$$|e_\ell - v_\ell|^{r'}_{W^{1,p}(\Omega)} + \beta \|e_\ell - v_\ell\|^2_{L^2(\Omega)} + |||I_\ell(v_\varepsilon + u_D)|||^2_\ell \lesssim \varepsilon \text{ for all } \ell \geqslant \ell_0.$$

A Cauchy inequality applied to the stabilisation norm proves

$$a_\ell(u_\ell, v_\ell) = -|||u_\ell|||^2_\ell + a_\ell(u_\ell, I_\ell(v_\varepsilon + u_D)) \leqslant -\frac{1}{2}|||u_\ell|||^2_\ell + \frac{1}{2}|||I_\ell(v_\varepsilon + u_D)|||^2_\ell.$$

Substitute $a_\ell(u_\ell, v_\ell)$ in Lemma 3.2 and add $\frac{1}{2}\|\!|u_\ell|\!\|_\ell^2$ on both sides. This leads to

$$\|\delta_\ell\|_{L^{p'}(\Omega)}^r + \beta\,\|e_\ell\|_{L^2(\Omega)}^2 + \|\!|u_\ell|\!\|_\ell^2 \lesssim \varepsilon \text{ for all } \ell \geqslant \ell_0. \qquad \square$$

Example 3.3. The two-well example from the computational benchmark [14] allows an estimate on $\|e_\ell\|_{L^2(\Omega)}$ even for $\beta = 0$. Let $n = 2$, let $F_1 := -F_2 := (3,2)/\sqrt{13}$, and let the energy density W be the convex hull of $F \mapsto |F - F_1|^2\,|F - F_2|^2$. That is

$$W(F) = \left(\max\left\{0, |F|^2 - 1\right\}\right)^2 + 4\left(|F|^2 - (3F(1) + 2F(2))^2/13\right). \tag{3.4}$$

Then [7, Lemma 9.1] proves, for all $v_\ell \in V_\ell$, that

$$\|e_\ell\|_{L^2(\Omega)}^2 \lesssim \int_\Omega \delta_\ell : \mathrm{D}e_\ell \,\mathrm{d}x + \|e_\ell - v_\ell\|_{H^1(\Omega)}^2.$$

Therefore, the arguments of Lemma 3.2 lead to

$$\|\delta_\ell\|_{L^{p'}(\Omega)}^r + \|e_\ell\|_{L^2(\Omega)}^2 \lesssim |e_\ell - v_\ell|_{W^{1,p}(\Omega)}^{r'} + \|e_\ell - v_\ell\|_{H^1(\Omega)}^2 + a_\ell(u_\ell, v_\ell).$$

This result can be used in the proof of Theorem 3.1 in order to obtain

$$\|\sigma - \sigma_\ell\|_{L^{p'}(\Omega)}^r + \|u - u_\ell\|_{L^2(\Omega)}^2 + \|\!|u_\ell|\!\|_\ell^2 \to 0 \text{ as } \ell \to \infty. \qquad \square$$

4 A Posteriori Error Estimates

Beyond the a posteriori error analysis of [18], the additional stabilisation term in the discretisation of this paper causes an additional difficulty in that the Galerkin orthogonality does *not* hold for the natural residual. Inspired from novell developments in the a posteriori error control of elliptic PDEs motivated by inexact solve [24, 16], this section presents some guaranteed upper error bound for the discretisation at hand for any approximation u_ℓ which does not necessarily satisfy (3.2) exactly. Thereby inexact solve is included.

Let $u \in \mathcal{A}$ solve (2.4) and let $u_\ell \in \mathcal{A}_\ell$ be arbitrary. It is *not* assumed that u_ℓ solves the discrete problem (2.6); the following theorem holds regardless of this. Recall the definitions of $\mathrm{osc}_{\ell,q}(\cdot)$ and Π_ℓ from Section 2 and, given $\sigma := \mathrm{D}W(\mathrm{D}u)$ and $\sigma_\ell := \mathrm{D}W(\mathrm{D}u_\ell)$, abbreviate

$$\Lambda_\ell := -2\beta(u_\ell - g) + f, \quad e_\ell := u - u_\ell \text{ and } \delta_\ell := \sigma - \sigma_\ell.$$

Theorem 4.1. *Given any $w_\ell \in W^{1,p}(\Omega;\mathbb{R}^m)$ with $w_\ell = u - u_\ell$ on the boundary $\partial\Omega$, and given any $\tau \in H(\mathrm{div}, \Omega; \mathbb{R}^{m\times n})$, it holds, for all $2 \leqslant q \leqslant p$ and for some constant $\varkappa$ known from [9, Lemma 3.5], that*

$$\begin{aligned}\varkappa/2\,\|\delta_\ell\|_{L^{p'}(\Omega)}^r + \beta\,\|e_\ell\|_{L^2(\Omega)}^2 &\leqslant (r\varkappa/2)^{1-r'}/r'\,|w_\ell|_{W^{1,p}(\Omega)}^{r'} + \beta\,\|w_\ell\|_{L^2(\Omega)}^2 \\ &+ \left(\|\sigma_\ell - \tau\|_{L^{q'}(\Omega)} + \|\Pi_\ell\Lambda_\ell + \mathrm{div}\,\tau\|_{L^{q'}(\Omega)} + \mathrm{osc}_{\ell,q'}(\Lambda_\ell)\right)\|e_\ell - w_\ell\|_{W^{1,q}(\Omega)}.\end{aligned}$$

Before the proofs conclude this section, some practical choice of τ in Theorem 4.1 is discussed as some Raviart-Thomas finite element functions in

$$RT_0(\mathcal{T}_\ell) := \left\{\tau_{\mathrm{RT}} \in P_1(\mathcal{T}_\ell) \cap H(\mathrm{div}, \Omega) : \forall T \in \mathcal{T}_\ell\ \exists a, b, c \in \mathbb{R}\ \forall x \in T, \tau_{\mathrm{RT}}(x) = (a, b) + cx\right\}.$$

We suggest the computation (or an accurate approximation) of

$$\mu_\ell := \min_{\tau\in RT_0(\mathcal{T}_\ell)^m} \left(\|\sigma_\ell - \tau\|_{L^{q'}(\Omega)} + \|\Pi_\ell\Lambda_\ell + \operatorname{div}\tau\|_{L^{q'}(\Omega)} \right)$$

and emphasise that any upper bound is allowed in Theorem 4.1. This leads to

$$\begin{aligned}\varkappa/2\,\|\delta_\ell\|^r_{L^{p'}(\Omega)} + \beta\,\|e_\ell\|^2_{L^2(\Omega)} \leqslant (r\varkappa/2)^{1-r'}/r'\,|w_\ell|^{r'}_{W^{1,p}(\Omega)} + \beta\,\|w_\ell\|^2_{L^2(\Omega)} \\ + \left(\mu_\ell + \operatorname{osc}_{\ell,q'}(\Lambda_\ell)\right)\|e_\ell - w_\ell\|_{W^{1,q}(\Omega)}\,.\end{aligned}$$

The algorithm of [6, Prop. 4.1] computes some w_ℓ from $(1-I_\ell)u_D$ with

$$\begin{aligned}\|w_\ell\|_{L^q(T)} &\approx h_T^{1/q}\,\|(1-I_\ell)u_D\|_{L^q(\partial T\cap\partial\Omega)} \quad\text{and} \\ \|\mathrm{D}w_\ell\|_{L^q(T)} &\lesssim h_T^{1/q-1}\,\|(1-I_\ell)u_D\|_{L^q(\partial T\cap\partial\Omega)} + h_T^{1/q}\,\|\partial(1-I_\ell)u_D/\partial s\|_{L^q(\partial T\cap\partial\Omega)}\,.\end{aligned} \tag{4.1}$$

(The proof of the second assertion is analogous to that of [6, Prop. 4.1] and the first is an immediate consequence of the design of w_ℓ.) This and $\|e_\ell - w_\ell\|_{W^{1,q}(\Omega)} \lesssim 1$ for bounded u_ℓ (i.e. solely $\|u_\ell\|_{W^{1,p}(\Omega)} \lesssim 1$ is assumed) lead to the practical estimate μ_ℓ as a computable guaranteed upper bound of the left-hand side of Theorem 4.1.

The choice $\tau = \sigma$ in Theorem 4.1 shows that the right-hand side is in fact optimal up to exponents. The reliability-efficiency gap of [14] is visible here in that we have no further estimate on $\|u_\ell\|_{W^{1,p}(\Omega)}$ [18, 14]. The following result indicates that μ_ℓ is sharp in the sense that it converges with the correct convergence rate. This theorem employs the Fortin interpolation operator $I_{\mathrm{F},\ell}$ defined for $\tau \in H(\operatorname{div},\Omega)\cap L^t(\Omega;\mathbb{R}^n)$ by $I_{\mathrm{F},\ell}\tau \in RT_0(\mathcal{T}_\ell)$ and

$$\fint_F n_F\cdot(1-I_{\mathrm{F},\ell})\tau\,\mathrm{d}s = 0 \quad\text{for all } F\in\mathcal{F}_\ell.$$

For the improved regularity of stress in the class of degenerate convex minimisation problems at hand, we refer to [17, 28].

Theorem 4.2 (Efficiency)**.** *If the exact stress σ allows the computation of some Fortin interpolant $\tau_\ell = I_{F,\ell}\sigma \in RT_0(\mathcal{T}_\ell;\mathbb{R}^{m\times n})$, it holds*

$$\|\sigma_\ell - \tau_\ell\|_{L^{q'}(\Omega)} + \|\Pi_\ell\Lambda_\ell + \operatorname{div}\tau_\ell\|_{L^{q'}(\Omega)} \lesssim \|\delta_\ell\|_{L^{q'}(\Omega)} + 2\beta\,\|e_\ell\|_{L^{q'}(\Omega)} + \|(1-I_{F,\ell})\sigma\|_{L^{q'}(\Omega)}\,.$$

It is expected that $\|(1-I_{\mathrm{F},\ell})\sigma\|_{L^{q'}(\Omega)} \lesssim \|h_\ell\,\mathrm{D}\sigma\|_{L^{q'}(\Omega)}$ (well known for $q=2$) and then the right-hand side of the assertion of Theorem 4.2 is of the form $(\text{error} + \mathcal{O}(H_\ell))$ and so converges with the (expected) optimal convergence rates.

Proof of Theorem 4.1. Let $\varkappa$ be the reciprocal of c_1 in [9, Lemma 3.5], which is also the multiplicative constant hidden in (3.3). Equation (3.3), the continuous Euler-Lagrange equation (3.1) and some carefull application of Young's inequality show, for $v = e_\ell - w_\ell \in V$, that

$$\begin{aligned}\varkappa\,\|\delta_\ell\|^r_{L^{p'}(\Omega)} + 2\beta\,\|e_\ell\|^2_{L^2(\Omega)} &\leqslant \int_\Omega (\delta_\ell : \mathrm{D}v + 2\beta e_\ell\cdot v)\,\mathrm{d}x + \int_\Omega (\delta_\ell : \mathrm{D}w_\ell + 2\beta e_\ell\cdot w_\ell)\,\mathrm{d}x \\ &\leqslant -\int_\Omega (\sigma_\ell : \mathrm{D}v - \Lambda_\ell\cdot v)\,\mathrm{d}x + \beta\,\|e_\ell\|^2_{L^2(\Omega)} + \beta\,\|w_\ell\|^2_{L^2(\Omega)} \\ &\quad + \varkappa/2\,\|\delta_\ell\|^r_{L^{p'}(\Omega)} + (r\varkappa/2)^{1-r'}/r'\,|w_\ell|^{r'}_{W^{1,p}(\Omega)}\,.\end{aligned}$$

Hence $\mathrm{Res}_\ell(v) := -\int_\Omega (\sigma_\ell : \mathrm{D}v - \Lambda_\ell \cdot v)\,\mathrm{d}x$ satisfies

$$\varkappa/2\,\|\delta_\ell\|_{L^{p'}(\Omega)}^r + \beta\,\|e_\ell\|_{L^2(\Omega)}^2 \leqslant \mathrm{Res}_\ell(v) + (r\varkappa/2)^{1-r'}/r'\,|w_\ell|_{W^{1,p}(\Omega)}^{r'} + \beta\,\|w_\ell\|_{L^2(\Omega)}^2.$$

Let $C_{q'}$ denote the Poincaré constant of convex domains with respect to the $W^{1,q'}$ norm. The fundamental theorem of calculus on some one-dimensional arc shows that $C_\infty \leqslant 1$. The paper [1] proves $C_1 = 1/2$. Hence, operator-interpolation arguments [8, 10] prove $C_{q'} \leqslant (1/2)^{1/q'} \leqslant 1$. The Poincaré inequality shows, for any $2 \leqslant q \leqslant p$, that

$$\begin{aligned}\int_\Omega (1-\Pi_\ell)\Lambda_\ell \cdot v\,\mathrm{d}x &= \int_\Omega h_\ell(1-\Pi_\ell)\Lambda_\ell \cdot \frac{1}{h_\ell}(1-\Pi_\ell)v\,\mathrm{d}x\\ &\leqslant \|h_\ell(1-\Pi_\ell)\Lambda_\ell\|_{L^{q'}(\Omega)}\,\|\mathrm{D}v\|_{L^q(\Omega)} = \mathrm{osc}_{\ell,q'}(\Lambda_\ell)\,\|\mathrm{D}v\|_{L^q(\Omega)}.\end{aligned}$$

For any $\tau \in H(\mathrm{div},\Omega;\mathbb{R}^{m\times n})$, the Hölder and Poincaré inequalities show

$$\begin{aligned}\mathrm{Res}_\ell(v) &= -\int_\Omega \big((\sigma_\ell - \tau) : \mathrm{D}v - (\Pi_\ell\Lambda_\ell + \mathrm{div}\,\tau)\cdot v - (1-\Pi_\ell)\Lambda_\ell \cdot v\big)\,\mathrm{d}x\\ &\leqslant \Big(\|\sigma_\ell - \tau\|_{L^{q'}(\Omega)} + \|\Pi_\ell\Lambda_\ell + \mathrm{div}\,\tau\|_{L^{q'}(\Omega)} + \mathrm{osc}_{\ell,q'}(\Lambda_\ell)\Big)\,\|v\|_{W^{1,q}(\Omega)}.\end{aligned}$$ □

Proof of Theorem 4.2. The triangle inequality yields

$$\|\sigma_\ell - \tau_\ell\|_{L^{q'}(\Omega)} \leqslant \|(1-I_{\mathrm{F},\ell})\sigma\|_{L^{q'}(\Omega)} + \|\delta_\ell\|_{L^{q'}(\Omega)}.$$

Since $f = 2\beta(u-g) - \mathrm{div}\,\sigma$, the commutative property $\mathrm{div}\,I_{\mathrm{F},\ell} = \Pi_\ell\,\mathrm{div}$ yields

$$\|\Pi_\ell\Lambda_\ell + \mathrm{div}\,\tau_\ell\|_{L^{q'}(\Omega)} = 2\beta\,\|\Pi_\ell e_\ell\|_{L^{q'}(\Omega)} \leqslant 2\beta\,\|e_\ell\|_{L^{q'}(\Omega)}.$$ □

5 Refined Analysis for an Interface Model Problem

This section is devoted for a model scenario from phase transition problems [14] with some solution u that is smooth outside some one-dimensional interface Γ. Suppose some (possibly non-unique) minimiser u of the continuous problem (2.4) satisfies $u \in W^{1,\infty}(\Omega;\mathbb{R}^m) \cap W^{2,p}(\Omega\backslash\Gamma;\mathbb{R}^m)$ for some finite union Γ of $(n-1)$ dimensional Lipschitz surfaces in $\overline{\Omega}$. Since Ω has a Lipschitz boundary, this implies Lipschitz continuity of u on Ω. We refer to [21] for sufficient conditions for $u \in W^{1,\infty}(\Omega;\mathbb{R}^m)$ and conclude that the remaining assumption $u \in W^{2,p}(\Omega\backslash\Gamma;\mathbb{R}^m)$ is the essential hypothesis expected in many interface problems. Let $u_\ell \in \mathcal{A}_\ell$ be the (unique) minimiser of the discrete stabilised problem (2.6). In the following, also $\Gamma = \varnothing$ is permitted to extend previous results [9] for highly regular minimisers.

We will abbreviate the set of all triangles that are touched by Γ as $\mathcal{T}_\ell(\Gamma) := \{T \in \mathcal{T}_\ell : \mathrm{dist}(T,\Gamma) = 0\}$, its cardinality as $|\mathcal{T}_\ell(\Gamma)|$, its union as $\Omega_{\Gamma,\ell} := \mathrm{int}(\bigcup \mathcal{T}_\ell(\Gamma))$ with volume $|\Omega_{\Gamma,\ell}|$ and its complement as $\Omega_{\Gamma,\ell}^{\mathrm{C}} := \Omega\backslash\overline{\Omega_{\Gamma,\ell}}$.

Theorem 5.1. *Provided $\beta > 0$, it holds*

$$\begin{aligned}\|\delta_\ell\|_{L^{p'}(\Omega)}^r + \|e_\ell\|_{L^2(\Omega)}^2 + |||u_\ell|||_\ell^2 &\lesssim H_\ell^{1+\gamma}\,|u|_{H^2(\Omega\backslash\Gamma)}^2 + H_\ell^2\,|u|_{W^{1,\infty}(\Omega)}^2\\ &\quad + H_\ell^{r/(r-1)}\,|u|_{W^{2,p}(\Omega_{\Gamma,\ell}^{\mathrm{C}})}^{r/(r-1)} + H_\ell^{\gamma+n-1}\,|u|_{W^{1,\infty}(\Omega)}^2\,|\mathcal{T}_\ell(\Gamma)| + |u|_{W^{1,\infty}(\Omega)}^{r/(r-1)}\,|\Omega_{\Gamma,\ell}|^{r/((r-1)p)}.\end{aligned}$$

Proof. With $w_\ell = (1 - I_\ell)e_\ell = (1 - I_\ell)u$, a Young inequality, (3.3) and [9, Theorem 3.8] yield

$$\|\delta_\ell\|_{L^{p'}(\Omega)}^r + \|e_\ell\|_{L^2(\Omega)}^2 + \|\!|u_\ell|\!\|_\ell^2 \lesssim |w_\ell|_{W^{1,p}(\Omega)}^{r/(r-1)} + \|w_\ell\|_{L^2(\Omega)}^2 + \|\!|I_\ell u|\!\|_\ell^2.$$

Theorem 4.4.4 in [10] shows $\|w_\ell\|_{L^2(\Omega)} \lesssim \|w_\ell\|_{L^\infty(\Omega)} \lesssim H_\ell\, |u|_{W^{1,\infty}(\Omega)}$ and

$$\begin{aligned} |w_\ell|_{W^{1,p}(\Omega)}^p &= |w_\ell|_{W^{1,p}(\Omega_{\Gamma,\ell})}^p + |w_\ell|_{W^{1,p}(\Omega_{\Gamma,\ell}^{\mathrm{C}})}^p \\ &\lesssim |u|_{W^{1,\infty}(\Omega_{\Gamma,\ell})}^p\, |\Omega_{\Gamma,\ell}| + H_\ell^p\, |u|_{W^{2,p}(\Omega_{\Gamma,\ell}^{\mathrm{C}})}^p. \end{aligned}$$

Let $\omega_F = \bigcup_{\substack{T\in\mathcal{T}_\ell \\ F\subset T}} T$ be the patch of a side $F \in \mathcal{F}_\ell$, and set $\mathcal{F}_\ell(\Gamma) = \{F \in \mathcal{F}_\ell(\Omega) : \omega_F \cap \Gamma \neq \varnothing\}$ and $\mathcal{F}_\ell^{\mathrm{C}}(\Gamma) = \mathcal{F}_\ell(\Omega)\backslash\mathcal{F}_\ell(\Gamma)$. Note that $[\mathrm{D}u]_F = 0$ for $F \in \mathcal{F}_\ell^{\mathrm{C}}(\Gamma)$. Then

$$\|\!|I_\ell u|\!\|_\ell^2 = H_\ell^{1+\gamma} \left(\sum_{F\in\mathcal{F}_\ell^{\mathrm{C}}(\Gamma)} h_F^{-1}\, \|[\mathrm{D}w_\ell]_F\|_{L^2(F)}^2 + \sum_{F\in\mathcal{F}_\ell(\Gamma)} h_F^{-1}\, \|[\mathrm{D}I_\ell u]_F\|_{L^2(F)}^2 \right).$$

The first sum can be estimated as in the proof of [9, Lemma 3.2], the second sum with

$$\|[\mathrm{D}I_\ell u]_F\|_{L^2(F)}^2 \lesssim h_F^{n-1}\, |I_\ell u|_{W^{1,\infty}(F)}^2 \leqslant h_F^{n-1}\, |u|_{W^{1,\infty}(F)}^2.$$

The observation $|\mathcal{F}_\ell(\Gamma)| \leqslant (n+1)\, |\mathcal{T}_\ell(\Gamma)|$ concludes the proof. □

Together with Theorem 5.1, the subsequent result implies strong convergence of the gradients in the model interface problem as $H_\ell \to 0$.

Theorem 5.2. *Under the aforementioned conditions on the (possibly non-unique) exact minimiser $u \in W^{1,\infty}(\Omega;\mathbb{R}^m) \cap W^{2,p}(\Omega\backslash\Gamma;\mathbb{R}^m)$, the error $e_\ell = u - u_\ell$ of the discrete solution $u_\ell \in \mathcal{A}_\ell$ of (2.6) satisfies*

$$\begin{aligned} \|\mathrm{D}e_\ell\|_{L^2(\Omega)} \lesssim{}& \|e_\ell\|_{L^2(\Omega)}^{1/3} + H_\ell^{5/6}\, \big\|\partial^2 u_D/\partial s^2\big\|_{L^2(\partial\Omega)}^{1/3} + H_\ell^{(1-\gamma)/2} \|\!|u_\ell|\!\|_\ell \\ &+ H_\ell^{-(1+\gamma)/4} \|\!|u_\ell|\!\|_\ell^{1/2} \left(\|e_\ell\|_{L^2(\Omega)}^{1/2} + H_\ell^{5/4}\, \big\|\partial^2 u_D/\partial s^2\big\|_{L^2(\partial\Omega)}^{1/2} \right). \end{aligned}$$

Proof. The basic idea of gradient control is the generalisation of the interpolation estimate $H^1(\Omega) = [L^2(\Omega), H^2(\Omega)]_{1/2}$ (from [8, 10]) for a reduced domain $\Omega\backslash\Gamma$. Let w_ℓ be the boundary value interpolation of $(1 - I_\ell)u_D$ as described in [6, Prop. 4.1], such that w_ℓ satisfies the inequalities in (4.1). A piecewise integration by parts shows, for $v := e_\ell - w_\ell \in W_0^{1,p}(\Omega;\mathbb{R}^m)$, that

$$\begin{aligned} \|\mathrm{D}e_\ell\|_{L^2(\Omega)}^2 &= \int_\Omega \mathrm{D}(u - u_\ell) : \mathrm{D}v \,\mathrm{d}x + \int_\Omega \mathrm{D}e_\ell : \mathrm{D}w_\ell \,\mathrm{d}x \\ &\leqslant \int_\Gamma v \cdot [\mathrm{D}u]_\Gamma\, n_\Gamma \,\mathrm{d}s - \int_{\Omega\backslash\Gamma} v \cdot \Delta u \,\mathrm{d}x - \sum_{F\in\mathcal{F}_\ell(\Omega)} \int_F v \cdot [\mathrm{D}u_\ell]_F\, n_F \,\mathrm{d}s + \|\mathrm{D}e_\ell\|_{L^2(\Omega)}\, \|\mathrm{D}w_\ell\|_{L^2(\Omega)}. \end{aligned}$$

The trace inequality on Γ and $|[\mathrm{D}u]_\Gamma\, n_\Gamma| \lesssim 1$ almost everywhere along Γ, lead to

$$\int_\Gamma v \cdot [\mathrm{D}u]_\Gamma\, n_\Gamma \,\mathrm{d}s \lesssim \|v\|_{L^2(\Gamma)} \lesssim \|v\|_{L^2(\Omega)} + \|v\|_{L^2(\Omega)}^{1/2}\, \|\mathrm{D}v\|_{L^2(\Omega)}^{1/2}.$$

The case $\Gamma = \varnothing$ is contained in [9, Theorem 4.4]. The piecewise Laplacian of u is bounded in $L^2(\Omega)$ and so (with the generic constant $C := \|\Delta u\|_{L^2(\Omega\backslash\Gamma)}$ hidden in the notation $C \approx 1$)

$$\int_{\Omega\backslash\Gamma} v \cdot \Delta u \,\mathrm{d}x \lesssim \|v\|_{L^2(\Omega)}.$$

The elementwise trace inequality [10, Theorem 1.6.6, p. 39] for an n-dimensional simplex T and one of its sides F, and $f \in W^{1,q}(T;\mathbb{R}^m)$, $1 \leqslant q < \infty$, reads

$$\|f\|_{L^q(F)}^q \lesssim h_T^{-1} \|f\|_{L^q(T)}^q + \|f\|_{L^q(T)}^{q-1} \|\mathrm{D}f\|_{L^q(T)} \lesssim h_T^{-1} \|f\|_{L^q(T)}^q + h_T^{q-1} \|\mathrm{D}f\|_{L^q(T)}^q .$$

The term $\int_F v \cdot [\mathrm{D}u_\ell]_F \, n_F \, \mathrm{d}s$ and the stabilisation $\|\!|u_\ell|\!\|_\ell$ are already analysed in the *Estimate on C* in the proof of [9, Theorem 4.4]. This results in

$$\sum_{F \in \mathcal{F}_\ell(\Omega)} \int_F v \cdot [\mathrm{D}u_\ell]_F \, n_F \, \mathrm{d}s \lesssim |\!|\!|u_\ell|\!|\!|_\ell \left(H_\ell^{(1-\gamma)/2} \|\mathrm{D}v\|_{L^2(\Omega)} + H_\ell^{-(1+\gamma)/2} \|v\|_{L^2(\Omega)} \right).$$

The proceeding estimates plus the absorbtion of $\|\mathrm{D}e_\ell\|_{L^2(\Omega)}$ lead to

$$\begin{aligned} \|\mathrm{D}e_\ell\|_{L^2(\Omega)}^2 &\lesssim \|v\|_{L^2(\Omega)} + \|v\|_{L^2(\Omega)}^{1/2} \|\mathrm{D}v\|_{L^2(\Omega)}^{1/2} + \|\mathrm{D}w_\ell\|_{L^2(\Omega)}^2 \\ &\quad + |\!|\!|u_\ell|\!|\!|_\ell \left(H_\ell^{(1-\gamma)/2} \|\mathrm{D}v\|_{L^2(\Omega)} + H_\ell^{-(1+\gamma)/2} \|v\|_{L^2(\Omega)} \right). \end{aligned}$$

The triangle inequality applied to $v = e_\ell - w_\ell$ and some careful elementary analysis to absorb $\|\mathrm{D}e_\ell\|_{L^2(\Omega)}^{1/2}$ eventually lead to

$$\begin{aligned} \|\mathrm{D}e_\ell\|_{L^2(\Omega)} &\lesssim \|e_\ell\|_{L^2(\Omega)}^{1/3} + \|w_\ell\|_{L^2(\Omega)}^{1/3} + |w_\ell|_{H^1(\Omega)} + H_\ell^{(1-\gamma)/2} |\!|\!|u_\ell|\!|\!|_\ell \\ &\quad + H_\ell^{-(1+\gamma)/4} |\!|\!|u_\ell|\!|\!|_\ell^{1/2} \left(\|e_\ell\|_{L^2(\Omega)} + \|w_\ell\|_{L^2(\Omega)} \right)^{1/2}. \end{aligned}$$

The inequalities (4.1), Poincaré and Friedrichs inequalities on sides $F \in \mathcal{F}_\ell(\partial\Omega)$ and removal of higher-order terms in H_ℓ conclude the proof. □

The following theorem is an improved a posteriori estimate based on Theorems 4.1 and 5.2.

Theorem 5.3. *Recall $u \in W^{1,\infty}(\Omega;\mathbb{R}^m) \cap W^{2,p}(\Omega\backslash\Gamma;\mathbb{R}^m)$, the definitions $e_\ell := u - u_\ell$ and $\delta_\ell := \sigma - \sigma_\ell$ for $\sigma := \mathrm{D}W(\mathrm{D}u)$ and $\sigma_\ell := \mathrm{D}W(\mathrm{D}u_\ell)$, and the definition of Λ_ℓ from Section 4. Set*

$$M(\tau) := \|\sigma_\ell - \tau\|_{L^2(\Omega)} + \|\Pi_\ell \Lambda_\ell + \operatorname{div} \tau\|_{L^2(\Omega)} + \operatorname{osc}_{\ell,2}(\Lambda_\ell) \quad \textit{for all } \tau \in H(\operatorname{div},\Omega;\mathbb{R}^{m\times n}).$$

Provided $\beta > 0$, it holds

$$\begin{aligned} \|\delta_\ell\|_{L^{p'}(\Omega)}^r + \|e_\ell\|_{L^2(\Omega)}^2 &\lesssim M(\tau)^{6/5} + H_\ell^{-(1+\gamma)/3} M(\tau)^{4/3} |\!|\!|u_\ell|\!|\!|_\ell^{2/3} \\ &\quad + M(\tau) \left(H_\ell^{(1-\gamma)/2} |\!|\!|u_\ell|\!|\!|_\ell + H_\ell^{1-\gamma/4} |\!|\!|u_\ell|\!|\!|_\ell^{1/2} \right) + H_\ell^{\min\{5,r'(1+1/p)\}} \qquad \textit{and} \\ \|\mathrm{D}e_\ell\|_{L^2(\Omega)}^2 &\lesssim M(\tau)^{2/5} + H_\ell^{-(1+\gamma)/9} M(\tau)^{4/9} |\!|\!|u_\ell|\!|\!|_\ell^{2/9} + H_\ell^{\min\{5/3,r'(1+1/p)/3\}} \\ &\quad + M(\tau)^{1/3} \left(H_\ell^{(1-\gamma)/2} |\!|\!|u_\ell|\!|\!|_\ell + H_\ell^{1-\gamma/4} |\!|\!|u_\ell|\!|\!|_\ell^{1/2} \right)^{1/3} + H_\ell^{1-\gamma} |\!|\!|u_\ell|\!|\!|_\ell^2 \\ &\quad + H_\ell^{-(1+\gamma)/2} |\!|\!|u_\ell|\!|\!|_\ell \left(M(\tau)^{6/5} + H_\ell^{-(1+\gamma)/3} M(\tau)^{4/3} |\!|\!|u_\ell|\!|\!|_\ell^{2/3} + H_\ell^{\min\{5,r'(1+1/p)\}} \right)^{1/2} \\ &\quad + H_\ell^{-(1+\gamma)/2} |\!|\!|u_\ell|\!|\!|_\ell M(\tau)^{1/2} \left(H_\ell^{(1-\gamma)/2} |\!|\!|u_\ell|\!|\!|_\ell + H_\ell^{1-\gamma/4} |\!|\!|u_\ell|\!|\!|_\ell^{1/2} \right)^{1/2}. \end{aligned}$$

Remark 5.4. Even in the case $\beta = 0$, strong convergence of gradients is possible. The theorem holds verbatim in Example 3.3 and in the modified two-well problem of Subsection 6.3.

Remark 5.5. The assertion of Theorem 5.3 holds for any discrete $u_\ell \in u_{D,\ell} + V_\ell$ which may approximate the discrete unique exact solution of (2.6). This allows the inexact SOLVE via an iterative procedure.

Proof of Theorem 5.3. Choose w_ℓ as in the proof of Theorem 5.2 and $q = 2$ in Theorem 4.1. Then (4.1) implies

$$\begin{aligned}\|\delta_\ell\|^r_{L^{p'}(\Omega)} + \|e_\ell\|^2_{L^2(\Omega)} &\lesssim M(\tau)\,\|e_\ell - w_\ell\|_{H^1(\Omega)} + |w_\ell|^{r'}_{W^{1,p}(\Omega)} + \|w_\ell\|^2_{L^2(\Omega)} \\ &\lesssim M(\tau)\left(|e_\ell|_{H^1(\Omega)} + \|e_\ell\|_{L^2(\Omega)} + H_\ell^{3/2}\right) + H_\ell^{\min\{5,r'(1+1/p)\}}.\end{aligned}$$

Theorem 5.2 yields an estimate on the semi-norm $|e_\ell|_{H^1(\Omega)}$. The absorbtion of $\|e_\ell\|_{L^2(\Omega)}$ then leads to the first assertion. The second assertion is an immediate consequence of the first one and Theorem 5.2. □

6 Numerical Experiments

This section illustrates the theoretical estimates and their impact on the reliability-efficiency gap on 2D benchmarks in computational microstructures [14, 4].

6.1 Numerical Algorithms

The adaptive finite element method (AFEM) and algorithmic details on the implementation in MATLAB in the spirit of [2] concern the state-of-the-art AFEM loop

$$\text{SOLVE} \to \text{ESTIMATE} \to \text{MARK} \to \text{REFINE}$$

and are explained below together with some notation.

6.1.1 SOLVE

The stabilised discrete problem (2.6) is solved in a nested iteration on a given triangulation $\mathcal{T}_\ell$ with MATLAB's standard-minimiser `fminunc` (with default tolerances). We set $\gamma = 1$ in the stabilisation term (2.5) in all our experiments. This is motivated by [9, Theorem 4.4] which suggest that $\gamma = 1$ yields an optimal convergence rate. The discrete solution of the previous AFEM loop iteration serves as a start vector for `fminunc`; for the first iteration, the initial vector is zero everywhere up to the Dirichlet boundary nodes. Since the Galerkin orthogonality is *not* required in Theorem 4.1, the termination of an iterative realisation for SOLVE is *not* a sensitive issue. In the computational PDEs, it is a fundamental issue to involve inexact solve. In this paper, however, the numerical examples are run with the standard settings of MATLAB.

6.1.2 ESTIMATE

The refinement indicator results from the error estimator of Theorem 4.1. The computation of the minimiser $\tau \in RT_0(\mathcal{T}_\ell)^m$ of

$$\|\sigma_\ell - \tau\|_{L^2(\Omega)} + \|\Pi_\ell \Lambda_\ell + \operatorname{div} \tau\|_{L^2(\Omega)} \tag{6.1}$$

runs Algorithm 6.1 based on the formula

$$a + b = \min_{s>0} \left((1+s)a^2 + (1+1/s)b^2\right) \quad \text{for } a, b > 0.$$

Input: σ_ℓ, $\Pi_\ell \Lambda_\ell$
$s_1 = 1$;
for $k = 1, 2, 3$ **do**
  Compute minimiser τ_k of
  $M(s_k, \tau) = (1 + s_k) \|\sigma_\ell - \tau\|^2_{L^2(\Omega)} + (1 + 1/s_k) \|\Pi_\ell \Lambda_\ell + \operatorname{div} \tau\|^2_{L^2(\Omega)}$;
  if $D^2_\tau M(\tau_k)$ *nearly singular (MATLAB "warning")* **then return** τ_k;
  $s_{k+1} = \|\Pi_\ell \Lambda_\ell + \operatorname{div} \tau_k\|_{L^2(\Omega)} / \|\sigma_\ell - \tau_k\|_{L^2(\Omega)}$;
  if $\max\left\{s_{k+1}, 1/s_{k+1}, \frac{|s_{k+1} - s_k|}{s_{k+1} + s_k}\right\} < \varepsilon_M^{0.8}$ **then return** τ_k;
Output: approximate flux τ

Algorithm 6.1: Approximate Flux Computation

The stopping criterion of Algorithm 6.1 monitors relative changes and avoids degenerate values of s. Undisplayed experiments have conviced us that a maxmium of three iterations and a stopping tolerance of $\varepsilon_{\mathrm{M}}^{0.8}$ (with the machine precision ε_{M}) yields satisfying results. The iteration is stopped whenever the s, $1/s$ or the relative change of s drops below this tolerance. As an additional precaution, the iteration also stops if the linear system is deemed "nearly singular" by MATLAB. Our experiments convinced us that ignoring this warning causes a breakdown with NaNs. Note that if $q \neq 2$, we still minimise the L^2 sums in (6.1) to avoid the computational cost of a nonlinear solve. With the computed minimiser τ, Section 4 yields the error estimator

$$\eta_{F,q'} := \|\sigma_\ell - \tau\|_{L^{q'}(\Omega)} + \|\Pi_\ell \Lambda_\ell + \operatorname{div} \tau\|_{L^{q'}(\Omega)} + \operatorname{osc}_{\ell,q'}(\Lambda_\ell).$$

This will be compared with the well-established *residual based a posteriori error estimator* [18]

$$\eta_{R,q'} := \left(\sum_{T \in \mathcal{T}_\ell} h_T^{q'} \|\Lambda_\ell\|^{q'}_{L^{q'}(T)}\right)^{1/q'} + \left(\sum_{F \in \mathcal{F}_\ell(\Omega)} h_F \|[\sigma_\ell]_F \cdot n_F\|^{q'}_{L^{q'}(F)}\right)^{1/q'}$$

as well as *averaging error control* [14]

$$\eta_{A,q'} := \|(1 - \Sigma_\ell)\sigma_\ell\|_{L^{q'}(\Omega)}$$

with the quasi interpolation operator Σ_ℓ with $(\Sigma_\ell \sigma_\ell)(z) := \fint_{\omega_z} \sigma_\ell(x)\,\mathrm{d}x$ for all nodes z of $\mathcal{T}_\ell$ followed by elementwise linear interpolation. The aforementioned error estimators are reliable for the original discretisation without stabilisation. The error estimators in Theorem 5.3 read

$$\begin{aligned}
\eta_{L,2} :=& \eta_{F,2}^{6/5} + H_\ell^{-(1+\gamma)/3} \eta_{F,2}^{4/3} |||u_\ell|||_\ell^{2/3} + \eta_{F,2} \left(H_\ell^{(1-\gamma)/2} |||u_\ell|||_\ell + H_\ell^{1-\gamma/4} |||u_\ell|||_\ell^{1/2}\right) + H_\ell^{\min\{5, r'(1+1/p)\}};\\
\eta_{H,2} :=& \eta_{F,2}^{2/5} + H_\ell^{-(1+\gamma)/9} \eta_{F,2}^{4/9} |||u_\ell|||_\ell^{2/9} + H_\ell^{\min\{5/3, r'(1+1/p)/3\}}\\
&+ \eta_{F,2}^{1/3} \left(H_\ell^{(1-\gamma)/2} |||u_\ell|||_\ell + H_\ell^{1-\gamma/4} |||u_\ell|||_\ell^{1/2}\right)^{1/3} + H_\ell^{1-\gamma} |||u_\ell|||_\ell^2\\
&+ H_\ell^{-(1+\gamma)/2} |||u_\ell|||_\ell \left(\eta_{F,2}^{6/5} + H_\ell^{-(1+\gamma)/3} \eta_{F,2}^{4/3} |||u_\ell|||_\ell^{2/3} + H_\ell^{\min\{5, r'(1+1/p)\}}\right)^{1/2}\\
&+ H_\ell^{-(1+\gamma)/2} |||u_\ell|||_\ell \eta_{F,2}^{1/2} \left(H_\ell^{(1-\gamma)/2} |||u_\ell|||_\ell + H_\ell^{1-\gamma/4} |||u_\ell|||_\ell^{1/2}\right)^{1/2}.
\end{aligned}$$

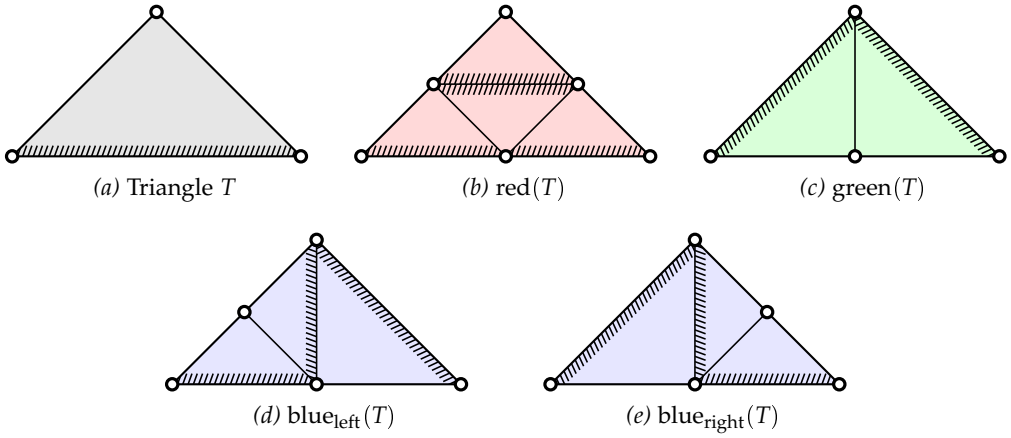

(a) Triangle T *(b)* red(T) *(c)* green(T) *(d)* blue$_{\text{left}}(T)$ *(e)* blue$_{\text{right}}(T)$

Figure 6.1: Possible refinements of a triangle T.

6.1.3 MARK

For any given $T \in \mathcal{T}_\ell$ with its set of faces $\mathcal{F}(T)$, $\partial T = \bigcup \mathcal{F}(T)$, and given τ from (6.1), set

$$\eta_F^{q'}(T) := \|\sigma_\ell - \tau\|_{L^{q'}(T)}^{q'} + \|\Pi_\ell \Lambda_\ell + \operatorname{div} \tau\|_{L^{q'}(T)}^{q'} + h_T^{q'} \|(1 - \Pi_\ell)\Lambda_\ell\|_{L^{q'}(T)}^{q'},$$
$$\eta_R^{q'}(T) := |T|^{q'/n} \|\Lambda_\ell\|_{L^{q'}(T)}^{q'} + |T|^{1/n} \sum_{F \in \mathcal{F}_\ell(\Omega) \cap \mathcal{F}(T)} \|[\sigma_\ell]_F \cdot n_F\|_{L^{q'}(F)}^{q'},$$
$$\eta_A^{q'}(T) := \|(1 - \Sigma_\ell)\sigma_\ell\|_{L^{q'}(T)}^{q'}.$$

Let $\eta^{q'}(T)$ be one of the refinement indicators $\eta_F^{q'}(T)$, $\eta_R^{q'}(T)$ or $\eta_A^{q'}(T)$. Some greedy algorithm computes $\mathcal{M}_\ell \subset \mathcal{T}_\ell$ of (almost) minimal cardinality such that

$$\sum_{T \in \mathcal{M}_\ell} \eta^{q'}(T) \leqslant 1/2 \sum_{T \in \mathcal{T}_\ell} \eta^{q'}(T).$$

6.1.4 REFINE

This step computes the smallest refinement $\mathcal{T}_{\ell+1}$ of $\mathcal{T}_\ell$ with $\mathcal{M}_\ell \subset \mathcal{T}_\ell \backslash \mathcal{T}_{\ell+1}$ based on the red-green-blue refinement strategy as illustrated in Figure 6.1. This refinement involves some closure algorithm to avoid hanging nodes.

6.2 Two-Well Benchmark of [14]

The computational microstructure benchmark of [14, Section 2] considers two wells with W from (3.4) in Example 3.3. The energy is given by (2.1) on the domain $\Omega = (0,1) \times (0,3/2) \subset \mathbb{R}^2$ with

$$g(x) := -3t^5/128 - t^3/3 \text{ and } u_D(x) := \begin{cases} g(x) & \text{for } t \leqslant 0, \\ t^3/24 + t & \text{for } t \geqslant 0 \end{cases}$$

for $t := (3(x_1 - 1) + 2x_2)/\sqrt{13}$; $p = q = 4$ and $f \equiv 0$. The unique minimiser u of $\min_{v \in \mathcal{A}} E(v)$ with $\mathcal{A} = u_D + W_0^{1,4}(\Omega)$ reads $u = u_D$ [14, Theorem 2.1] and $\beta = 1$ allows for Theorems 5.1–5.3 to hold. An initial triangulation $\mathcal{T}_0$ is given by a criss triangulation of $(0,1) \times (0,3/2)$ with 12

congruent triangles and the two interior nodes $(1/2, 1/2)$ and $(1/2, 1)$. The adaptive algorithm of Subsection 6.1 computes a sequence of discrete solutions $(u_\ell)_\ell$ and stresses $(\sigma_\ell)_\ell$, as well as error estimators η_F, η_R and η_A with and without stabilisation for uniform and adaptive meshes and led to Figure 6.2 with overall observations of Subsection 6.7. The empirical convergence rates for uniform and R- as well as F-adapted mesh-refining are collected in Table 6.1. Note that the error estimator η_L performs better than η_F. This is evident from the table for uniform mesh refinements, but a closer look at Figure 6.2 reveals that even in the adaptive scenarios, η_L converges slightly faster than η_F. This is in accordance to the theory of Section 5 where η_L is derived from η_F based on additional smoothness assumptions.

6.3 Modified Two-Well Benchmark

This subsection concerns a modification of the previous problem with (3.4) and a linear right-hand side for $\beta = 0$ and $f(x) := -\operatorname{div}(\mathrm{D}W(\mathrm{D}u_D(x)))$ and unique solution $u = u_D$ as before. Note that Example 3.3 applies to this problem, and so the proof of Theorem 3.1 yields

$$\|\sigma - \sigma_\ell\|_{L^{p'}(\Omega)}^r + \|u - u_\ell\|_{L^2(\Omega)}^2 + |||u_\ell|||_\ell^2 \to 0 \text{ as } \ell \to \infty$$

and Theorems 5.1–5.3 hold as well. The algorithms of Subsection 6.1 ran with and without stabilisation for uniform and adaptive meshes with the same initial triangulation as in Subsection 6.2 and led to Figure 6.3 with overall observations of Subsection 6.7. The empirical convergence rates for uniform and R- as well as F-adapted mesh-refining are collected in Table 6.1 for completeness although they are empirical identical with those observed in Subsection 6.2.

6.4 Three-Well Benchmark

The energy density W of [4, Example 5.9.3, p. 72] is the convex hull of $\min\{|F|^2, |F-(1,0)|^2, |F-(0,1)|^2\}$ with explicit form in [4, Example 5.6.4, p. 58]. Let furthermore $\Omega = (0,1)^2 \subset \mathbb{R}^2$ and $u_D(x_1, x_2) := a(x_1 - 1/4) + a(x_2 - 1/4)$ with $a(t) := t^3/6 + t/8$ for $t \leqslant 0$ and $a(t) := t^5/40 + t^3/8$ for $t \geqslant 0$. Then the energy is given by (2.1) with $\beta = 0$ and $f := -\operatorname{div} \mathrm{D}W(\mathrm{D}u_D)$. The exact solution $u = u_D$ satisfies the interface condition of Section 5 and allows Theorem 5.2 to hold. Theorems 5.1 and 5.3 do not apply because $\beta = 0$. As initial triangulation $\mathcal{T}_0$ we use the coarsest criss triangulation $\mathcal{T}_0 = \{\operatorname{conv}\{(0,0),(1,0),(1,1)\}, \{(0,0),(1,1),(0,1)\}\}$ of the unit square.

The algorithms of Subsection 6.1 ran with and without stabilisation for uniform and adaptive meshes and led to Figure 6.4 with overall observations of Subsection 6.7. Beyond those general conclusions, this example demonstrates the difficulties with ill-conditioned Hessians. While the unstabilised method reaches 10^6 degrees of freedom without difficulty on uniform meshes, the adapted algorithms fail without stabilisation beyond 260059 degrees of freedom (η_F-adaptive) and 52340 degrees of freedom (η_R-adaptive). MATLAB's error message "Input to EIG must not contain NaN or Inf" indicates that a matrix operation returned non-finite numbers let `fminunc` break down. Undisplayed numerical experiments show condition numbers up to 10^{10} and beyond. The error estimator η_A fails to predict the error of the stabilised stress $\|\sigma - \sigma_\ell\|_{L^2(\Omega)}$. The empirical convergence rates for uniform and R- as well as F-adapted mesh-refining are collected in Table 6.1. The inconclusive convergence of $\|u - u_\ell\|_{L^2(\Omega)}$ (adaptive) and $\|\mathrm{D}(u - u_\ell)\|_{L^2(\Omega)}$ without stabilisation consists of oscillations until 1000 degrees of freedom followed by no further convergence at all. It appears unreasonable to assign a meaningful slope to those graphs.

6.5 An Optimal Design Example

The energy density of the topology optimisation problem of [13, 17, 5, 31, 29, 27, 25] reads

$$W(F) := \phi(|F|) \text{ for } F \in \mathbb{R}^2 \text{ with } \phi(t) := \lambda/2 + \begin{cases} t^2 & \text{for } 0 \leqslant t \leqslant \sqrt{\lambda}, \\ 2\sqrt{\lambda}(t - \sqrt{\lambda}/2) & \text{for } \sqrt{\lambda} \leqslant t \leqslant 2\sqrt{\lambda}, \\ t^2/2 + \lambda & \text{for } t \geqslant 2\sqrt{\lambda}. \end{cases}$$

This leads to problem (2.4) with $\beta = 0$, $\lambda = 0.0084$, $u_D \equiv 0$ and two different choices

$$f \equiv 1 \text{ (Figure 6.6) and } f = -\operatorname{div} DW(Du) \text{ for } u(x_1, x_2) = x_1 x_2 (1 - x_1)(1 - x_2) \text{ (Figure 6.5).}$$

The smooth solution u that corresponds to the latter choice of f permits for the application of Theorem 5.2. Since regularity of the solutions corresponding to the former choice of f is unclear, only the results of Sections 3–4 apply. As initial triangulation $\mathcal{T}_0$, we use the coarsest criss triangulation $\mathcal{T}_0 = \{\operatorname{conv}\{(-1,-1),(1,-1),(1,1)\}, \{(-1,-1),(1,1),(-1,1)\}\}$ of $\Omega = (-1,+1)^2$.

The algorithms of Subsection 6.1 ran with and without stabilisation for uniform and adaptive meshes and led to Figures 6.6–6.5 with the overall observations of Subsection 6.7. The empirical convergence rates for uniform and R- as well as F-adapted mesh-refining are collected in Table 6.1. The inconclusive convergence of $\|u - u_\ell\|_{L^2(\Omega)}$ for adaptive mesh-refinements without stabilisation (marked as "—") consists of oscillations without a clear trend beyond 1000 degrees of freedom. For uniform meshes the unstabilised error $\|u - u_\ell\|_{L^2(\Omega)}$ shows only a short range of (strong) convergence (up to 1000 degrees of freedom).

6.6 Empirical Convergence Rates

Global convergence without regularity assumptions. Theorem 3.1 asserts that $\|u - u_\ell\|_{L^2(\Omega)}$, $\|\sigma - \sigma_\ell\|_{L^p(\Omega)}$, and $|||u_\ell|||_\ell$ all tend to zero as $H_\ell \to 0$. The plain convergence result applies to all examples from Subsections 6.2–6.5 for the uniform mesh-refinements with $H_{\ell+1} = H_\ell/2$. The numerical experiments, however, show empirical convergence rates displayed in the first columns of Table 6.1. The adaptive algorithms do not reflect the condition $H_\ell \to 0$ explicitly and hence convergence is not guaranteed a priori. Undisplayed investigations show that indeed in the R-adapted version of the three-well example of Subsection 6.4, this condition $H_\ell \to 0$ does not appear to be true for more than 4585 degrees of freedom. In all other experiments we observe convergence rates even for unstabilised discretisations.

Empirical convergence rates for interface model problems. Theorem 5.1 provides an a priori error estimate and an estimate of the stabilisation norm. It applies to the benchmark of Subsections 6.2–6.3 only, because of $\beta > 0$ and Example 3.3, and the smoothness conditions imposed upon u from Section 5. Recall the definitions of $\mathcal{T}_\ell(\Gamma)$, $\Omega_{\Gamma,\ell}$ and $\Omega^{\mathrm{C}}_{\Gamma,\ell}$ from Section 5 and assume $\|u\|_{L^2(\Omega\setminus\Gamma)} \approx 1 \approx \|u\|_{W^{2,p}(\Omega^{\mathrm{C}}_{\Gamma,\ell})}$, $|\mathcal{T}_\ell(\Gamma)| \approx H_\ell^{-1}$ and $|\Omega_{\Gamma,\ell}| \approx H_\ell$ in this discussion. This leads to a convergence rate of $H_\ell^{2/p}$ for the right-hand side of Theorem 5.1. The observed convergence rates of $\|\sigma - \sigma_\ell\|_{L^{p'}(\Omega)}$, $\|u - u_\ell\|_{L^2(\Omega)}$ and $|||u_\ell|||_\ell$ for the stabilised benchmark examples in Table 6.1 show convergence rates beyond those guaranteed in Theorem 5.1 even in Subsections 6.2–6.3 and 6.5.

Theorem 5.2 implies, up to perturbations on the boundary,

$$\|D(u - u_\ell)\|_{L^2(\Omega)} \lesssim \|u - u_\ell\|^{1/3}_{L^2(\Omega)} + |||u_\ell|||_\ell + H_\ell^{1/2} |||u_\ell|||_\ell^{1/2} \|u - u_\ell\|^{1/2}_{L^2(\Omega)}.$$

Example of Subsection		$\|\sigma-\sigma_\ell\|^r_{L^{r'}(\Omega)}$ unstab.	stab.	$\|u-u_\ell\|^2_{L^2(\Omega)}$ unstab.	stab.	$\|\|\|u_\ell\|\|\|^2_\ell$ unstab.	stab.	η_R unstab.	η_F stab.	η_L stab.	$\|\mathrm{D}(u-u_\ell)\|^2_{L^2(\Omega)}$ unstab.	stab.	η_H stab.
6.2	unif	5/3	5/3	3/2	3/2	3	3	4/5	4/5	1	1/2	1/2	(1/2)
	R-adapt	(2)	4/3	(2)	1	3/2	9/4	1	1	1	2/3	(2/5)	(1/2)
	F-adapt	(2)	4/3	(2)	1	(4)	9/4	1	1	1	2/3	(2/5)	(1/2)
6.3	unif	5/3	5/3	3/2	3/2	3	3	4/5	4/5	1	1/2	1/2	(1/2)
	R-adapt	(2)	4/3	(2)	1	(3/2)	9/4	1	1	1	2/3	(2/5)	(1/2)
	F-adapt	(2)	4/3	(2)	1	(4)	9/4	1	1	1	2/3	(2/5)	(1/2)
6.4	unif	2	(1)	(8/3)	(2)	2	7/2	1	1	4/3	—	(2/5)	(1/2)
	R-adapt	2	0	—	0	—	(0)	1	0	0	—	0	0
	F-adapt	2	6/5	—	1	—	2	1	4/5	1	—	1/3	(1/3)
6.5	unif	2	2	—	(10/3)	4	4	1	1	3/2	2	2	(6/5)
$f \not\equiv 1$	R-adapt	2	2	—	3	11/3	11/3	1	1	7/4	(2)	2	(4/3)
	F-adapt	2	2	—	7/3	11/3	3	1	1	7/4	2	2	(4/3)
6.5	unif					7/2	7/2	1	1	4/3			(2/3)
$f \equiv 1$	R-adapt					10/3	7/2	1	1	6/5			(2/3)
	F-adapt					7/2	4	1	1	6/5			(2/3)

Table 6.1: Observed convergence rates in Figures 6.2–6.5 for uniform and adaptive mesh refining. Convergence rates are given as powers of the representative mesh-size $1/\sqrt{\mathrm{ndof}}$ which is proportional to H_ℓ on uniform grids. Unavailable values are left blank, non-continuous rates are put in parantheses, inconclusive convergence behaviour is marked by "—".

Since the exact solutions of Subsections 6.2–6.4 are all smooth up to a one-dimensional interface line, Theorem 5.2 applies to these examples. Table 6.1 shows that the right-hand side of Theorem 5.2 is dominated by $\|u-u_\ell\|_{L^2(\Omega)}$ in all examples with uniform refinements and that the inequality $\|\mathrm{D}(u-u_\ell)\|_{L^2(\Omega)} \lesssim \|u-u_\ell\|_{L^2(\Omega)}^{1/3}$ is satisfied by all those examples (except the three-well benchmark).

Reliability without regularity assumptions. Up to boundary terms, Theorem 4.1 states

$$\|\sigma-\sigma_\ell\|_{L^{p'}(\Omega)}^2 + \beta\,\|u-u_\ell\|_{L^2(\Omega)}^2 \lesssim \eta_F\,\|u-u_\ell\|_{W^{1,p}(\Omega)}\,.$$

The convergence rates confirm this assertion for the general and rough estimate $\|u-u_\ell\|_{W^{1,p}(\Omega)} \lesssim 1$ in the sense that the rates for η_F are worse than or equal to those of $\|\sigma-\sigma_\ell\|_{L^{p'}(\Omega)}^2$ and $\|u-u_\ell\|_{L^2(\Omega)}^2$. In the numerical examples, $\|u-u_\ell\|_{H^1(\Omega)}$ is computed and displayed in Table 6.1 and the convergence rates of the product $\|u-u_\ell\|_{H^1(\Omega)}\,\eta_F$ can be compared with those of $\|\sigma-\sigma_\ell\|_{L^{p'}(\Omega)}^2 + \|u-u_\ell\|_{L^2(\Omega)}^2$. This comparison confirms the above a posteriori error estimate. In the examples with $p=2$ (of Subsections 6.4–6.5), there holds even equality of the convergence rates which demonstrates the efficiency of the estimate of Theorem 4.1.

Efficiency without regularity assumptions. Up to oscillations and the (possibly) higher-order term $\|(1-I_{\mathrm{F},\ell})\sigma\|_{L^{q'}(\Omega)}$, Theorem 4.2 states

$$\eta_F \lesssim \|\sigma-\sigma_\ell\|_{L^{p'}(\Omega)} + \beta\,\|u-u_\ell\|_{L^p(\Omega)}\,.$$

The displayed convergence rates of Table 6.1 confirm this estimate.

Reliability of the refined a posteriori error control. Theorem 5.3 applies to the example of Subsection 6.2 and states

$$\|\sigma-\sigma_\ell\|_{L^{p'}(\Omega)}^2 + \|u-u_\ell\|_{L^2(\Omega)}^2 \lesssim \eta_L \quad\text{and}\quad \|\mathrm{D}(u-u_\ell)\|_{L^2(\Omega)}^2 \lesssim \eta_H.$$

At first glance, Table 6.1 displays convergence rates for $\|\mathrm{D}(u-u_\ell)\|_{L^2(\Omega)}^2$ and η_H like $2/5$ and $1/2$ for the adaptive mesh-refinements in Subsections 6.2–6.3. This seems to be in contradiction to the overall reliability $\|\mathrm{D}(u-u_\ell)\|_{L^2(\Omega)}^2 \lesssim \eta_H$ of Theorem 5.3. A closer look at Figures 6.2–6.3 reveals that, in fact, $\|\mathrm{D}(u-u_\ell)\|_{L^2(\Omega)}^2$ is up to two orders of magnitude smaller than η_H and so clearly supports Theorem 5.3. The convergence rates of η_H displayed in Table 6.1 surpass those of $\eta_F^{2/5} \leqslant \eta_H$. However, the convergence history plots of η_H indicate that the higher-order terms in the definition of η_H dominate in a large preasymptotic range. Therefore they are denoted in parantheses in Table 6.1.

All displayed convergence rates of η_L are better or at least equal to those of η_F. For instance, for uniform mesh-refining in Subsections 6.2–6.3, the error terms $\|\sigma-\sigma_\ell\|_{L^{p'}(\Omega)}^2 + \|u-u_\ell\|_{L^2(\Omega)}^2$ converge with the empirical convergence rate $5/3$ while the upper bound η_F does so with a reduced convergence rate $4/5$. The refined error estimator η_L is a guaranteed upper bound (via Theorem 5.3) and converges with an empirical convergence rate 1.

Performance of the minimisation algorithm 6.1. In all numerical experiments of this paper, Algorithm 6.1 reaches the maximal number 3 of iterations. While this suggests that the optimal s is *not* found after three iterations, undisplayed experiments with higher iteration counts and hence higher computational efforts result solely in marginal improvements.

6.7 Global Observations and Conclusions

Effects of stabilisation. The empirical convergence rates of the error estimators η_F, η_R, η_A and the errors $\|u - u_\ell\|_{L^2(\Omega)}$ and $\|\sigma - \sigma_\ell\|_{L^{p'}(\Omega)}$ for uniform mesh-refinement with and without stabilisation coincide. This indicates that the choice $\gamma = 1$ leads to some significant perturbation but maintains the correct convergence rate at the same time. This is different for adaptive mesh refinement with less optimal convergence rates. Our conclusion is that an improved adaptive algorithm has to be developed with balance of local mesh-refinement and global stabilisation parameters in future research. The tested algorithm from Subsection 6.1 does neither reflect the effects of stabilisation nor that of inexact solve.

Another important aspect of the stabilisation is the regularisation of the Hessian in the step SOLVE of Subsection 6.1. In the three-well problem of Subsection 6.4, the unstabilised adaptive algorithms fail.

Adaptive versus uniform mesh-refinement. The overall empirical convergence rates of the errors and estimators of the unstabilised computation for adaptive mesh-refinements are better than those for uniform mesh-refinements. This is in contrast to the stabilised computation, where the true errors $\|\sigma - \sigma_\ell\|_{L^{p'}(\Omega)}$ and $\|u - u_\ell\|_{L^2(\Omega)}$ behave better for uniform compared with the two adaptive mesh-refinments (with the exception in Subsection 6.5 where there is equality). It is observed that adaptivity does not necessarily improve the converegnce rates of the error $\|\sigma - \sigma_\ell\|_{L^{p'}(\Omega)}$ and $\|u - u_\ell\|_{L^2(\Omega)}$ in a stabilised computation. Surprisingly, the convergence of the gradient errors $\|\mathrm{D}(u - u_\ell)\|_{L^2(\Omega)}$are indeed improved in the instabilised calculation by adaptive mesh-refinements. The adaptive mesh-refinement is expected to reduce the a posteriori error estimators in the first place: cf. [19, 12] for the estimator reduction property. Indeed, the convergence rates of the a posteriori error estimators η_R, η_F, η_L, η_H are improved (or optimal) for adaptive mesh-refinements (except for the three-well example of Subsection 6.4).

Strong convergence of the gradients. The convergence of the gradient error of the stabilised problem surpasses the expectations of [9] in Subsection 6.5 but fails to do so in Subsections 6.2–6.3. The improved error estimator η_H shows the same convergence rate as the error of the gradients in Subsections 6.2–6.4. This holds for uniform and for adapted mesh refinements and suggests that η_H is in fact reliable and efficient for $\beta > 0$.

Guaranteed error control. The assertion on η_F in Theorem 4.1 is reflected in the numerical examples in that the stress approximations converge faster than η_F in all cases. This suggests that the estimate $\|u - u_\ell\|_{W^{1,p}(\Omega)} \lesssim 1$ is by far too pessimistic. In fact, the optimal design example with known exact solution fulfils $\|\sigma - \sigma_\ell\|^2_{L^2(\Omega)} \approx \eta_F \|u - u_\ell\|_{H^1(\Omega)}$. In this sense, the estimate of Theorem 4.1 is sharp. Similar affirmative conclusions follow for Theorem 4.2 and 5.3.

Reliability-efficiency gap. In comparison with the residual-based error estimator of [18, 14], the new a posteriori error estimators η_L and η_H of Theorem 5.3 lead to refined error control. The improvement is marginal for uniform meshes without stabilisation but significant for adaptive stabilised computations. η_L matches the convergence of the errors and so narrows the reliability-efficiency gap.

References

[1] G. Acosta and R. G. Durán, *An optimal Poincaré inequality in L^1 for convex domains*, Proc. Amer. Math. Soc., 132 (2004), pp. 195–202.

[2] J. Alberty, C. Carstensen, and S. A. Funken, *Remarks around 50 lines of Matlab: short finite element implementation*, Numer. Algorithms, 20 (1999), pp. 117–137.

[3] J. M. Ball and R. D. James, *Proposed experimental tests for the theory of fine microstructures and the two-well problem*, Phil. Trans R. Soc. Lond., A 338 (1992), pp. 389–450.

[4] S. Bartels, *Numerical Analysis of Some Non-Convex Variational Problems*, Ph.D. thesis, Christian-Albrechts Universität zu Kiel, Kiel, Germany, 2001. `http://eldiss.uni-kiel.de/macau/receive/dissertation_diss_00000519`.

[5] S. Bartels and C. Carstensen, *A convergent adaptive finite element method for an optimal design problem*, Numer. Math., 108 (2007), pp. 359–385.

[6] S. Bartels, C. Carstensen, and G. Dolzmann, *Inhomogeneous Dirichlet conditions in a priori and a posteriori finite element error anylysis*, Numer. Math., 99 (2004), pp. 1–24.

[7] S. Bartels, C. Carstensen, P. Plecháč, and A. Prohl, *Convergence for stabilisation of degenerate convex minimsation problems*, IFB, 6 (2004), pp. 253–269.

[8] J. Bergh and J. Löfstrom, *Interpolation spaces*, Springer-Verlag, Berlin, 1976.

[9] W. Boiger and C. Carstensen, *On the strong convergence of gradients in stabilised degenerate convex minimisation problems*, SIAM J. Numer. Anal., 47 (2010), pp. 4569–4580.

[10] S. C. Brenner and L. Scott, *The mathematical theory of finite element methods. 2nd ed.*, Texts in Applied Mathematics. 15. Berlin: Springer. xv, 361 p, 2002.

[11] C. Carstensen, *Clément interpolation and its role in adaptive finite element error control*, in Partial Differential Equations and Functional Analysis, E. Koelink, J. M. v. Neerven, B. d. Pagter, and G. H. Sweers, eds., Birkhäuser Verlag, 2006, pp. 27–43.

[12] ——, *Convergence of an adaptive fem for a class of degenerate convex minimisation problems*, IMA J. Numer. Anal., 28 (2008), pp. 423–439.

[13] C. Carstensen, D. Günther, and H. Rabus, *Adaptive mixed finite element method for an optimal design problem*, (2011). Submitted.

[14] C. Carstensen and K. Jochimsen, *Adaptive finite element methods for microstructures? numerical experiments for a 2-well benchmark*, Computing, 71 (2003), pp. 175–204.

[15] C. Carstensen and R. Klose, *Guaranteed a posteriori finite element error control for the p-Laplace problem*, SIAM J. Sci. Comput., 25 (2003), pp. 792–814.

[16] C. Carstensen and C. Merdon, *Five variations of the Luce-Wohlmuth a posteriori error control*, (2011). In preparation.

[17] C. Carstensen and S. Müller, *Local stress regularity in scalar non-convex variational problems*, SIAM J. Math. Anal., 34 (2002), pp. 495–509.

[18] C. Carstensen and P. Plecháč, *Numerical solution of the scalar double-well problem allowing microstructure*, Math. Comp., 66 (1997), pp. 997–1026.

[19] J. M. Cascon, C. Kreuzer, R. H. Nochetto, and K. G. Siebert, *Quasi-optimal convergence rate for an adaptive finite element method*, SIAM J. Numer. Anal., 46 (2008), pp. 2524–2550.

[20] M. Chipot, *Elements of nonlinear analysis*, Birkhäuser Advanced Texts. Basel: Birkhäuser. vi, 2000.

[21] M. Chipot and L. C. Evans, *Linearisation at infinity and Lipschitz estimates for certain problems in the calculus of variations*, Proc. R. Soc. Edinburgh A, 102 (1986), pp. 291–303.

[22] P. G. Ciarlet, *The Finite Element Method for Elliptic Problems*, Society for Industrial Mathematics, April 2002.

[23] B. Dacorogna, *Direct methods in the calculus of variations. 2nd ed.*, Applied Mathematical Sciences 78. Berlin: Springer. xii, 2008.

[24] L. El Alaoui, A. Ern, and M. Vohralík, *Guaranteed and robust a posteriori error estimates and balancing discretization and linearization errors for monotone nonlinear problems*, Comp. Meth. Appl. Mech. Eng., 200 (2011), pp. 2782–2795.

[25] R. Glowinski, J.-L. Lions, and R. Trémolières, *Numerical analysis of variational inequalities*, vol. 8 of Studies in Mathematics and its Applications, North-Holland Publishing Co., Amsterdam, 1981.

[26] J. Goodman, R. V. Kohn, and L. Reyna, *Numerical study of a relaxed variational problem from optimal design*, Comput. Methods Appl. Mech. Eng., 57 (1986), pp. 107–127.

[27] B. Kawohl, J. Stará, and G. Wittum, *Analysis and numerical studies of a problem of shape design*, Arch. Rational Mech. Anal., 114 (1991), pp. 349–363.

[28] D. Knees, *Global stress regularity of convex and some nonconvex variational problems*, Ann. Mat. Pura Appl. (4), 187 (2008), pp. 157–184.

[29] R. V. Kohn and G. Strang, *Optimal design and relaxation of variational problems I–III*, Comm. Pure Appl. Math., 39 (1986), pp. 113–137,139–182,353–377.

[30] S. Müller, *Variational models for microstructure and phase transisions*. Hildebrandt, S. (ed.) et al., Calculus of variations and geometric evolution problems. Lectures given at the 2nd session of the Centro Internazionale Matematico Estivo (CIME), Cetraro, Italy, June 15-22, 1996. Berlin: Springer. Lect. Notes Math. 1713, 85-210 (1999)., 1999.

[31] F. Murat and L. Tartar, *Calcul des variations et homogénéisation*, in Homogenization methods: theory and applications in physics, D. B. et al., ed., vol. 57 of Collect. Dir. Études Rech. Élec. France, Eyrolles, Paris, 1985, pp. 319–369.

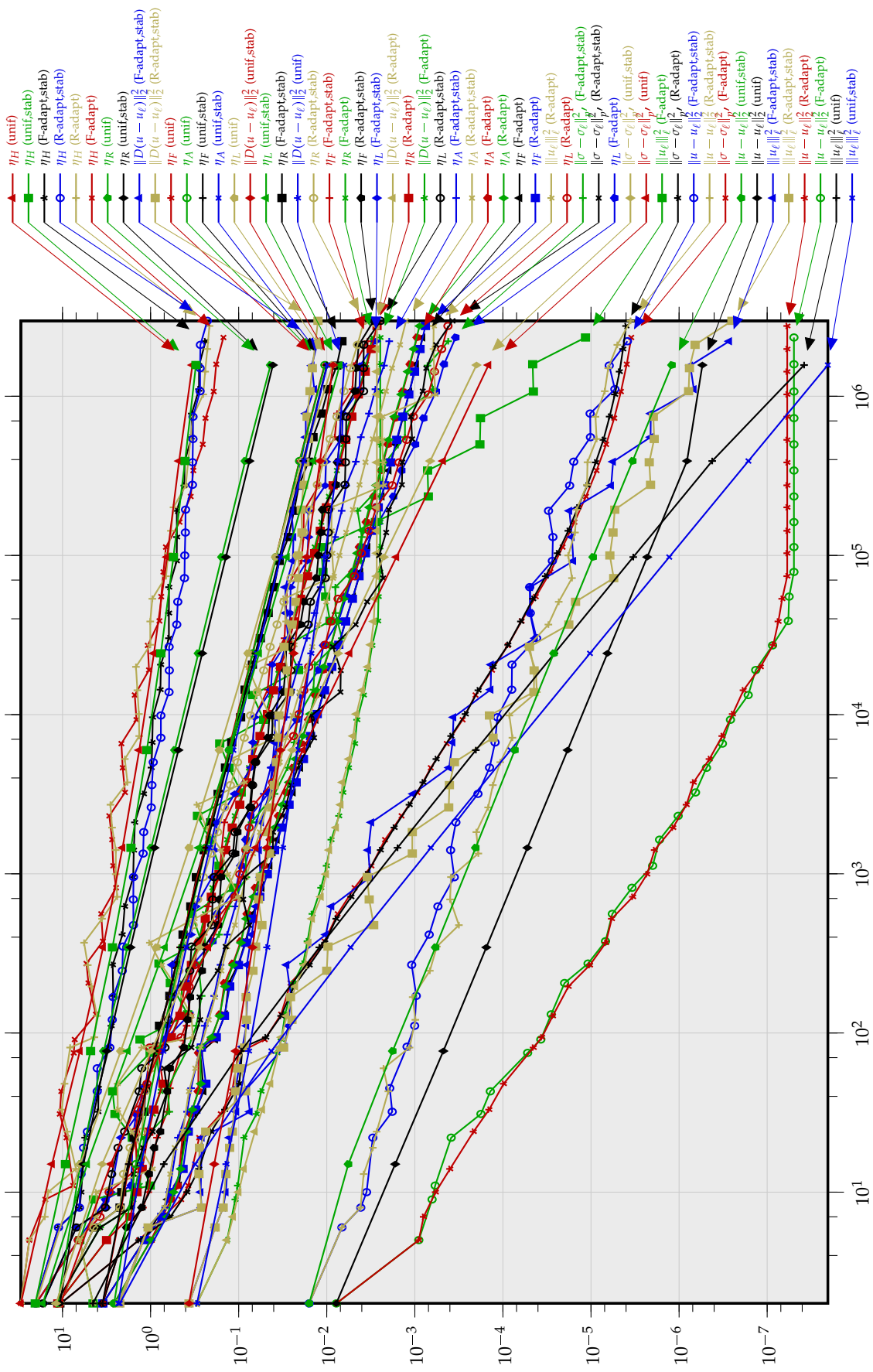

Figure 6.2: Errors and error estimators of the two-well benchmark of Subsection 6.2, plotted against the number of degrees of freedom

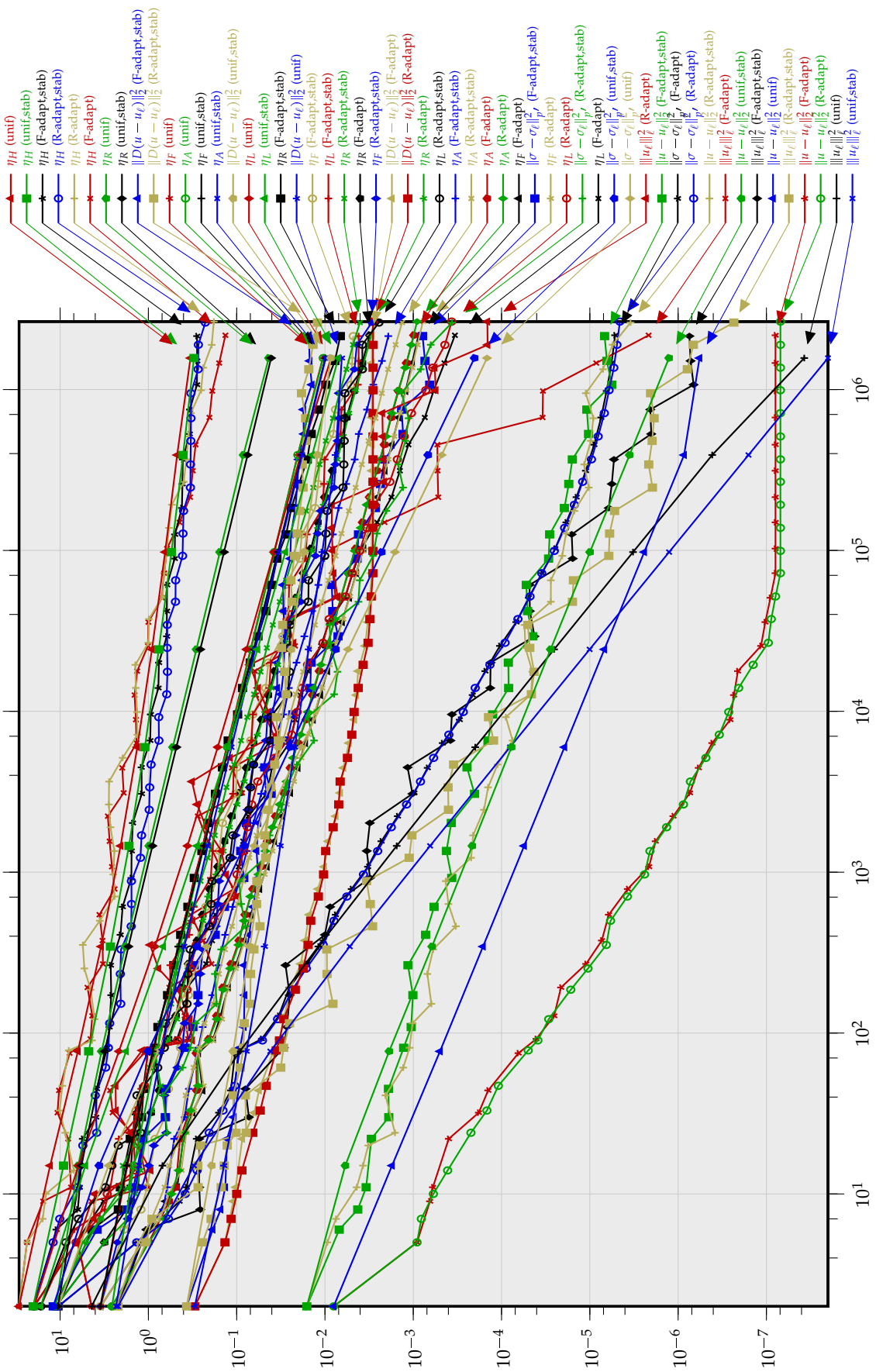

Figure 6.3: Errors and error estimators of the modified two-well benchmark of Subsection 6.3, plotted against the number of degrees of freedom

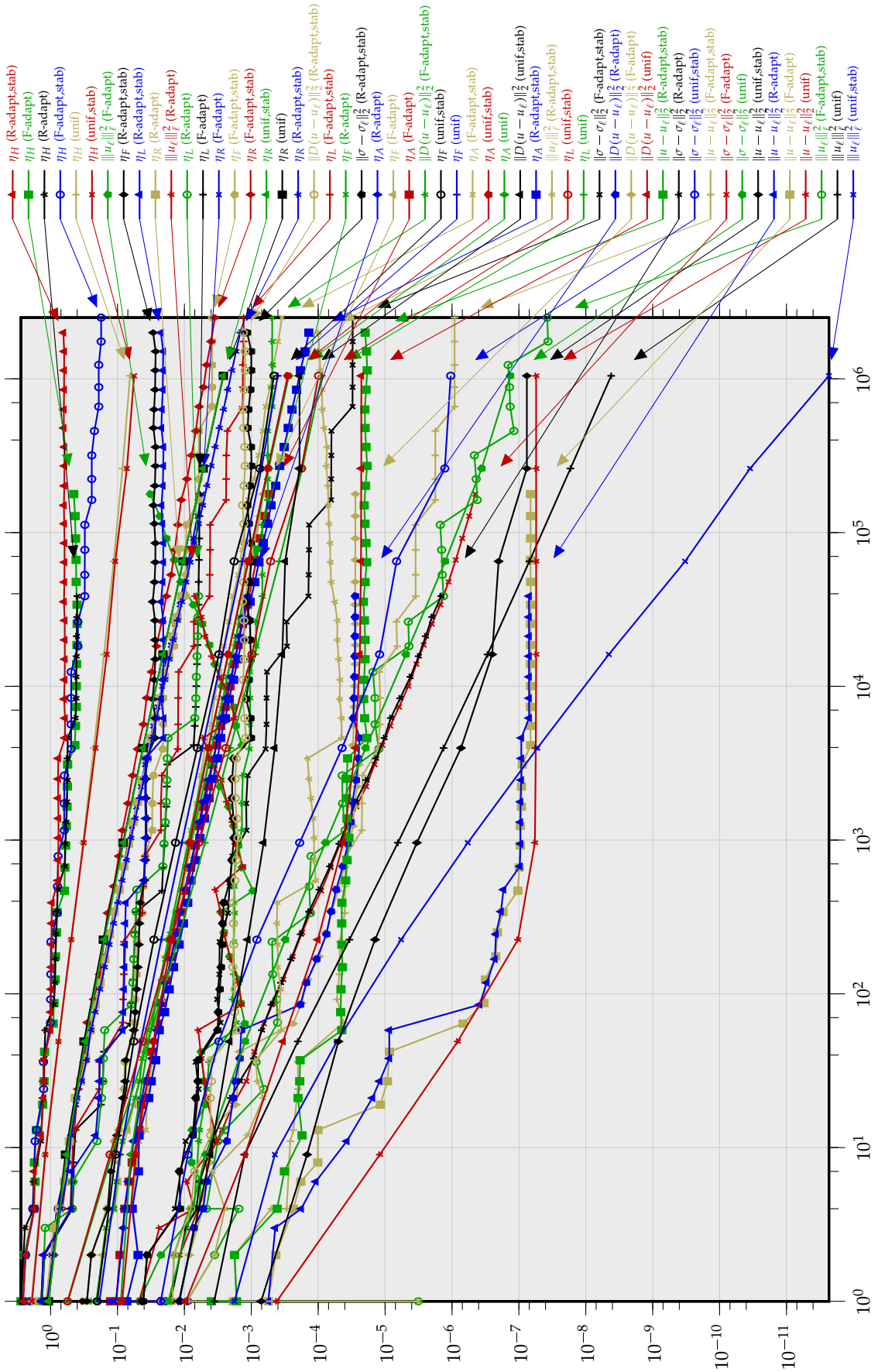

Figure 6.4: Errors and error estimators of the three-well benchmark of Subsection 6.4, plotted against the number of degrees of freedom

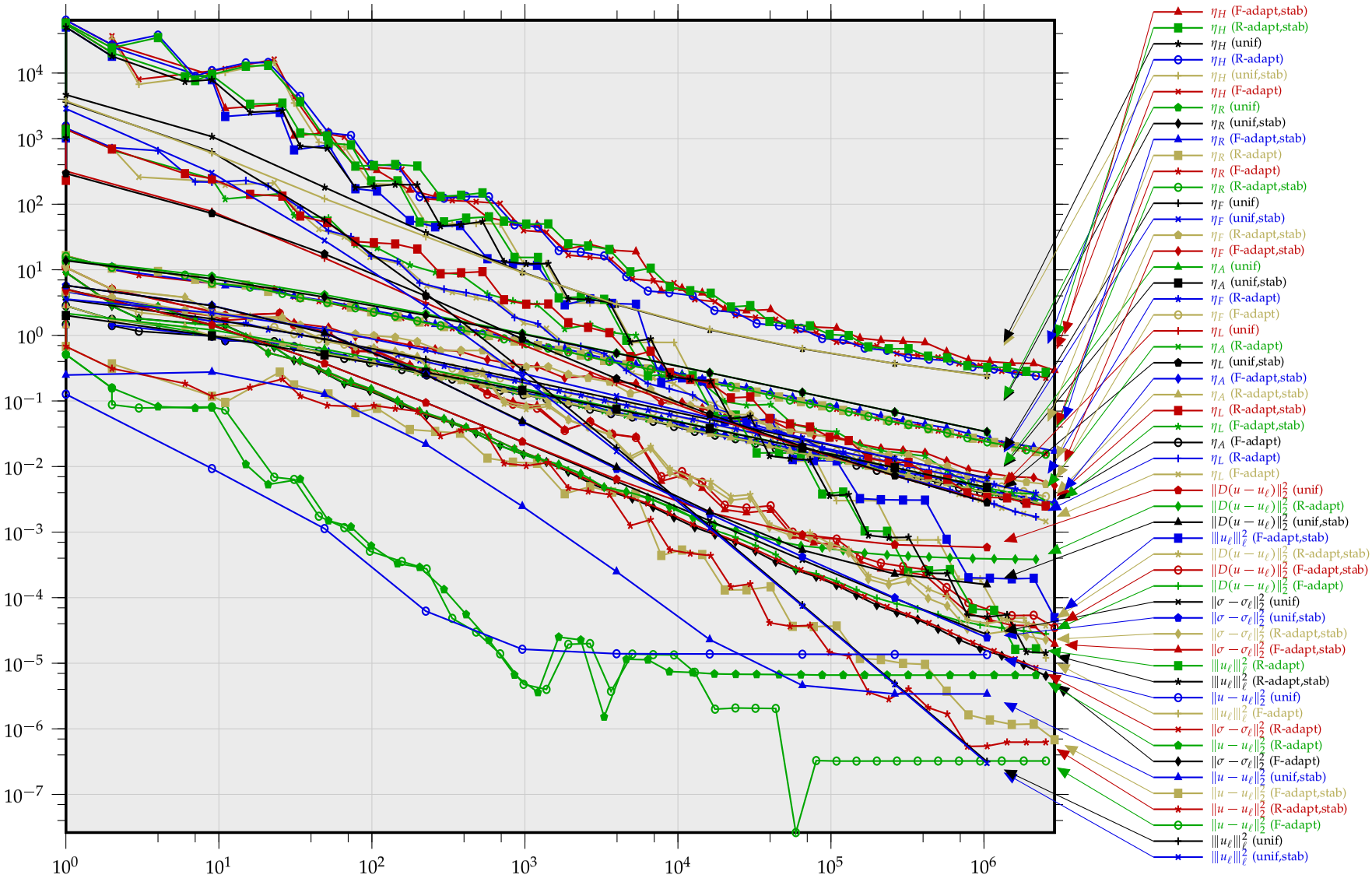

Figure 6.5: Errors and error estimators of the optimal design example of Subsection 6.5 with $u_D(x_1, x_2) = x_1x_2(1-x_1)(1-x_2)$, plotted against the number of degrees of freedom

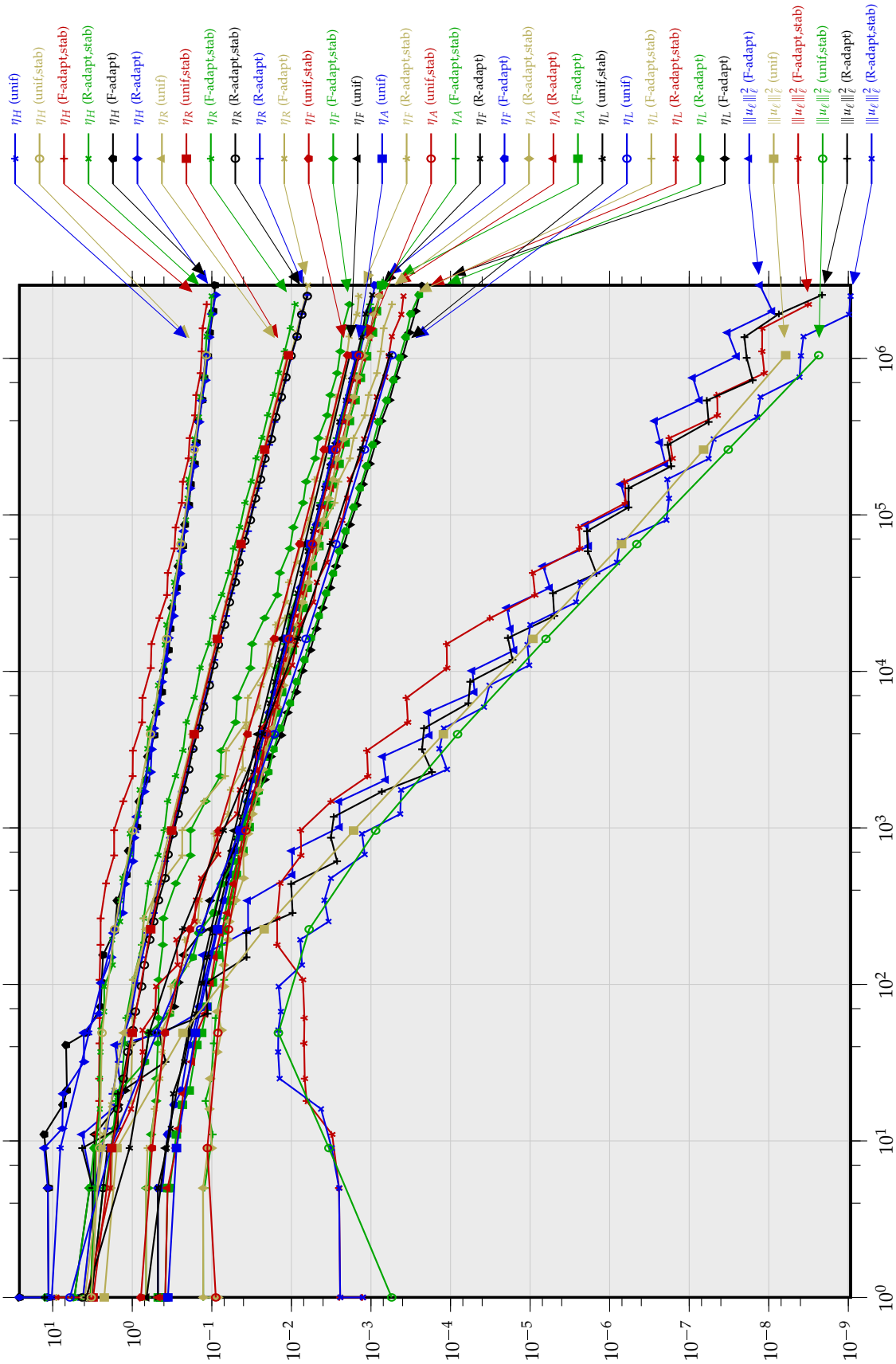

Figure 6.6: Error estimators of the optimal design example of Subsection 6.5 with $f \equiv 1$, plotted against the number of degrees of freedom